POLITECNICO DI TORINO

Master's Degree in Aerospace Engineering

Master's Degree Thesis

Structural Composite Material with Novel Cellulose Fibre Reinforcement

Supervisors

Prof. Marco GHERLONE

Prof. Malin AKERMO

Candidate

Mauro Antonio MURRONE

April 2024

Abstract

In recent decades, the necessity to find a completely environmentally friendly substitute for synthetic fibres in composite applications has intensified, driven by the objective of reducing emissions in both the production and disposal of composite components. Natural fibres present a potential solution, yet they have some issues such as the inhomogeneous quality of their cross-section and mechanical properties, depending on different aspects, for example, growing conditions and the amount of intake water. Another potential solution is organic man-made fibres, such as fibre made from Cellulose NanoFibrils, which do not present the previously cited drawbacks. This thesis investigates and compares the potentials of organic fibres, either man-made or natural, in composite reinforcement applications. To accomplish this, organic fibres are integrated into composite plates using two distinct thermoset matrices, epoxy and vinyl ester, respectively via methods of hot pressing and vacuum infusion. Subsequently, the produced composite plates undergo tensile testing, with the results being compared with the theoretical values. Furthermore, microscopy is employed to examine the adhesion at the interface between reinforcement and matrix. The findings indicate that man-made fibres from Cellulose NanoFibrils bind more efficiently with thermoset matrices compared to flax fibres, making them more adept as reinforcement materials for thermoset composites.

keywords

Composite material, organic man-made fibres, natural fibres, thermosets matrices, vacuum infusion, hot pressing.

Sammanfattning

Under de senaste decennierna har behovet av att hitta en helt miljövänlig ersättning för syntetiska fibrer i kompositapplikationer intensifierats, drivet av målet att minska utsläppen både vid produktion och avfallshantering av kompositkomponenter. Naturliga fibrer presenterar en potentiell lösning, men de har vissa problem som den ojämna kvaliteten på deras tvärsnitt och mekaniska egenskaper, beroende på olika aspekter, till exempel växtförhållanden och mängden intaget vatten. En annan potentiell lösning är organiska konstgjorda fibrer, som fibrer tillverkade av cellulosa nanofibriller, som inte har de tidigare nämnda nackdelarna. Denna avhandling undersöker och jämför potentialen hos organiska fibrer, antingen konstgjorda eller naturliga, i kompositförstärkningsapplikationer. För att uppnå detta integreras organiska fibrer i kompositplattor med hjälp av två olika termohärdande matriser, epoxi och vinyl-ester, via metoder för varmpressning och vakuuminfusion. Därefter genomgår de producerade kompositplattorna dragprovning, med resultaten jämförda med de teoretiska värdena. Dessutom används mikroskopi för att undersöka vidhäftningen vid gränssnittet mellan förstärkning och matris. Resultaten indikerar att konstgjorda fibrer från cellulosa nanofibriller binder effektivare med termohärdande matriser jämfört med linfibrer, vilket gör dem mer lämpliga som förstärkningsmaterial för termohärdande kompositer.

Nyckelord

Kompositmaterial, organiska konstgjorda fibrer, naturlig fiber, termohärdande matriser, vakuuminfusion, varmpressning.

Sommario

Negli ultimi decenni, la necessità di trovare un sostituto completamente ecologico alle fibre sintetiche nei materiali compositi si è intensificata, spinta dall'obiettivo di ridurre le emissioni sia nella produzione che nello smaltimento dei componenti dei materiali compositi. Le fibre naturali rappresentano un possibile sostituto alle fibre sintetiche, ma presentano alcuni problemi come l'inomogeneità della loro sezione trasversale e delle proprietà meccaniche, le quali dipendono da diversi aspetti, come le condizioni di crescita e la quantità di acqua assorbita. Un'altra possibile alternativa è l'utilizzo di fibre organiche artificiali, come le fibre prodotte da NanoFibrille di Cellulosa, che non presentano gli svantaggi precedentemente citati. Questa tesi investiga e confronta le potenzialità delle fibre organiche, sia artificiali che naturali, come rinforzo dei materiali compositi. Per fare ciò, le fibre organiche sono integrate in materiali compositi con due matrici termoindurenti distinte, resina epossidica ed estere vinilico, rispettivamente tramite metodi di pressatura a caldo e infusione sottovuoto. Successivamente, i materiali compositi prodotti vengono sottoposti a test di trazione, confrontando i risultati ottenuti con i valori teorici. Inoltre, la microscopia viene utilizzata per esaminare l'adesione all'interfaccia tra rinforzo e matrice. Dai risultati si evince che le fibre artificiali di NanoFibrille di Cellulosa si legano in modo più efficiente alle matrici termoindurenti rispetto alle fibre di lino, rendendole più idonee come rinforzo per i materiali compositi.

Parole chiave

Materiali compositi, fibre organiche sintetiche, fibre naturali, matrici termoindurenti, infusione sottovuoto, pressatura a caldo.

Acknowledgements

I would like to express my sincere gratitude to my supervisor at KTH, Malin Akermo not only for her guidance during my thesis but for sharing with me her knowledge about composite materials. I really learned a lot from working with her.
I appreciate the participation of Dan Zenkert in my thesis project, I thank him for every important suggestion given to me.
I would like to express my gratitude to my supervisor at Polito, Marco Gherlone, for following my activities and for his support during my thesis.
I would like to thank Karl Hakansson and Anna Wiberg for giving me the opportunity to work with them and letting me study the Cellulextreme product.
Special thanks to Monica Norrby and Anders Beckman for their assistance during the laboratory activities.
Finally, I would like to say thank you to all the people in the Lightweight Structure departments who helped me with my thesis project.

Table of Contents

List of Tables

List of Figures

Acronyms

PAN
Polyacrylonitrile

GHG
Greenhouse gas

CNF
Cellulose NanoFibril

MMF
Man Made Fibres

VE
Vinyl Ester

E
Epoxy

VIP
Vacuum Infusion Process

FVR
Fibre Volume Ratio

PA
Polyamide

PLA
Poly-Lactic Acid

PP

Polypropylene

HR

Humidity Relative

Chapter 1

Introduction

Synthetic man-made fibres, such as glass and carbon fibres, have dominated the structural composites market, widely used across various industries including aerospace, automotive, and marine, thanks to their elevated specific stiffness and strength [1]. The primary issue with these fibres lies in their production: they are manufactured from nonrenewable petroleum resources, such as polyacrylonitrile (PAN) for carbon fibres or silica (SiO_2), resulting in higher carbon dioxide (CO_2) emissions, a greenhouse gas (GHG) contributing to the global warming [2]. The increasing pollution and fossil fuel depletion have led to the search for alternative and lower environmental impact fibres for composite materials.
A potential solution to this environmental issue is to substitute synthetic fibres with those derived from natural sources such as wood, animals, leaves, and grasses in composite applications. Nowadays, these natural fibres are extensively used not only for their environmental advantages but also for their considerable mechanical properties and lightweight nature. However, one of their primary drawbacks lies in their inconsistent quality [3].
Cellulose fibre, an organic man-made fibre, represents another possible solution to this environmental problem thanks to the abundant available sources and their good mechanical properties, which are homogeneous concerning those of natural fibres. Cellulose is the most abundant natural polymer on Earth; indeed, its production is estimated to be 10^{11}–10^{12} tons per year [4]. Furthermore, it is a renewable, biodegradable, and non-toxic material. Cellulose is extracted from wood and silk in the form of nanosized fibrils (CelluloseNanoFibrils CNF) through chemical and mechanical treatments [5]. The crystalline structure of cellulose imparts CNF with excellent mechanical properties (Young's modulus of 130-150 GPa and strength of 1.0-3.0 GPa [6]) making them a suitable building block for high-performance biomaterial fibres. Flow-based assembly is a method for the fabrication of cellulose fibres from CNF. It succeeds in densely packaging the aligned CNF fibres together into a macroscale structure and efficiently transferring stress among the fibrils,

providing the macrostructure of the fibre with elevated mechanical properties (highest recorded stiffness around 70 GPa and strength around 1.32 GPa) [7]. Celluxtreme is a startup based in Stockholm, Sweden, that aims to use innovative technologies and methodologies to replace fossil-based products with sustainable and renewable alternatives. Employing flow-based assembly and green chemistry, to produce fully biodegradable and renewable CNF fibre, minimizing CO_2 emissions to a minimum during manufacturing.

1.1 Aim of the work

This thesis aims to compare how man-made cellulose fibre and natural fibre interact with different thermosets matrices in structural composite processes. The manufactured composites are required to have a volume fraction of fibres suitable for load-bearing applications, ranging from 50 to 55%. Two manufacturing techniques have been employed in composite: hot pressing with epoxy film and vacuum infusion with vinyl ester resin. Furthermore, the adhesion between hydrophilic fibres and the hydrophobic matrix has been analyzed in the microscopy of the cross-section. Once the composites have been produced, the tensile test was performed to evaluate their mechanical properties and compare them to the theoretical values.

Chapter 2

Theoretical Background

2.1 Composite material

Composite material is defined as a combination of two or more different constituents, each possessing distinct chemical and physical properties. This blending results in a material that showcases enhanced properties in comparison to the individual components used independently. Unlike metal alloys, where the components are dissolved within each other at a microscopic level, in composite materials, the components are macroscopically separated from each other [8].
In structural applications, composites typically consist of a bulk phase called the matrix, which encloses a fibrous reinforcing phase known as the reinforcement. The matrix transfers the load to the fibres and protects them from environmental effects. In addition, it gives the composites their shape, surface appearance, and environmental tolerance. While the fibres bear the majority of the load and provide the material with stiffness and strength [9].
This type of composite can be classified according to the type of its matrix or its reinforcements. The matrix can be categorized as polymeric, ceramic, or metallic. The reinforcements can be classified as discontinuous ("short fibre") or continuous ("long fibres"), and they can be randomly or aligned [9]. This thesis focuses on studying composites with long and aligned fibres embedded in a polymeric matrix.

2.2 Fibre

The fibres employed in reinforced polymeric composites can be categorized into two groups:

- **Natural fibres** are fibres produced by nature. They can be classified into diverse groups based on their origin, including animal fibres such as wool and silk, mineral fibres, and plant fibres such as bast, leaf, seed, wood, and grasses.

- **Man-made fibre (MMF)** are fibres created by humans. MMF can be organic or inorganic. Organic MMFs are derived from natural materials like wood, while inorganic MMFs are produced from synthetic materials such as glass and carbon [10].

Figure 2.1 illustrates the classification of fibres, showcasing the various types within each group.

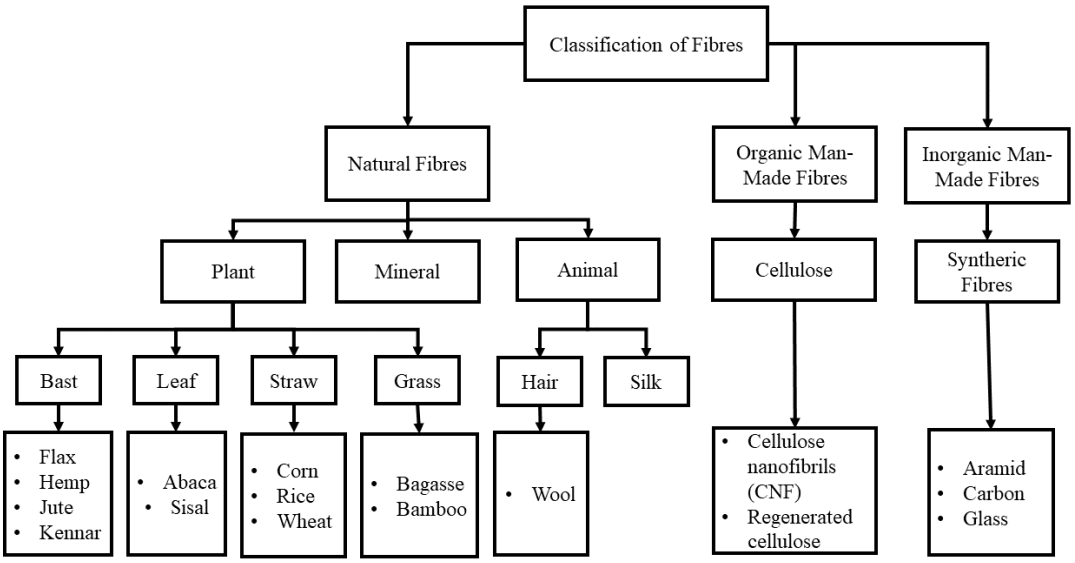

Figure 2.1: Schematic representation of fibre classification [10].

The main advantage of synthetic fibres is their excellent mechanical properties, which remain high even at elevated temperatures. This characteristic, combined with their strong cohesion with polymeric matrices, positions them as the most commonly utilized composite reinforcements in load-bearing applications. However, synthetic fibres have significant drawbacks that cannot be neglected: a high price, difficulty recycling, and they are produced from nonrenewable resources. In contrast, natural fibres are biodegradable and are cost-effective as composite reinforcements. Nevertheless, the utilization of natural fibres in structural composites is currently limited due to several issues. Their low resistance to high temperatures and to ultraviolet light, but the most critical issue is their hydrophilic behaviour. This behaviour leads to dimensional instability and inhomogeneous quality, meaning that the mechanical properties and dimensions depend on the climatic and growing conditions, as well as the amount of absorbed water [11]. Additionally, natural fibres exhibit incompatibility with hydrophobic polymer matrices, which are the

most commonly used in structural composite applications [3]. Organic MMF can be considered an intermediate group between natural and synthetic fibres since it exhibits characteristics of both. Like natural fibres, they are plant-based, which gives them hydrophilic behaviour. They are manufactured using processes similar to synthetic fibres. As a result, their mechanical properties could be superior to those of natural fibres and are not influenced by climatic and growing environments. The cellulose nanofibrils (CNF) fibres represent the highest-performing fibres in this group. Table 2.1 provides an overview of the main advantages and disadvantages of these three fibre categories. While Table 2.2 shows the physical properties of different fibres.

Table 2.1: Comparison of different types of fibres, the first two rows are taken from paper [3].

Fibre	**Advantages**	**Disadvantages**
Natural fibre	Biodegradable Low density/price	Inhomogeneous quality Water sensitive Incompatibility with the hydrophobic matrix
Synthetic fibre	Moisture resistance Good mechanical properties	Produced from nonrenewable resource Difficult in recycling Relative high price
CNF fibre	Homogeneous quality Biodegradable Low density	Water sensitive Incompatibility with the hydrophobic matrix

Table 2.2: Comparison between physical properties of different fibres.

Fibre & **Reference**	**Density** (kg/m^3)	**Young's modulus** (GPa)	**Tensile strength** (MPa)	**Elongation at break** (%)
CNF [7]	1500	70	1320	5-6
Flax [3]	1530	58 ± 15	1339 ± 486	3.27
Hemp [3]	1520	70	920	1.7
E-glass [9]	2570-2600	69-72	3450-3790	4.5-4.9
Kevlar49(aramid) [9]	1440	131	3600-4100	2.8
Carbon(HS/S) [9]	1700-1900	160-250	1400-4930	0.8-1.9
SiC [9]	2700-3300	45-480	0.3-4.9	0.6-1

2.2.1 Flax fibres

Linum usitatissimum, commonly known as flax, is a flowering plant that belongs to the Linaceae family. Flax is cultivated for its seeds and fibre. The seeds are used for producing oil (linseed oil) and flour, while the fibre is processed into textiles known as linen. In recent years, the use of flax fibres as reinforcement materials in polymeric matrix composites has increased, especially for structural applications.

Chemical composition

The main chemical constituents of the plant fibres are:

- **Cellulose**, represented by the chemical formula $(C_6H_{10}O_5)_n$, is a polysaccharide composed of numerous glucose molecules (ranging from 10,000 to 15,000) linked together through glycosidic bonds. This molecular structure is illustrated in Figure 2.2. The cellulose structure has a high level of crystallinity thanks to the presence of the Hydroxyl group (-OH), three for each repeating unit. These hydroxyl groups form hydrogen bonds between different monomers, resulting in a regular and linear structure that imparts strength and rigidity to cellulose [12]. Additionally, the hydroxyl groups in cellulose have a good affinity with water molecules, which give a hydrophilic nature to the plants and, consequently, to their derived fibres [10].
- **Hemicellulose** is a natural polymer composed of carbohydrate monomers. It possesses a branched and open structure that enables it to attract a greater number of water molecules [13].
- **Lignin** is an amorphous, highly complex polymer primarily composed of phenylpropane units. It, along with pectin [14], serves to bind cellulose and hemicellulose together in plant fibres [15].
- **Wax** influences wettability and the adhesion between fibre and matrix [10].

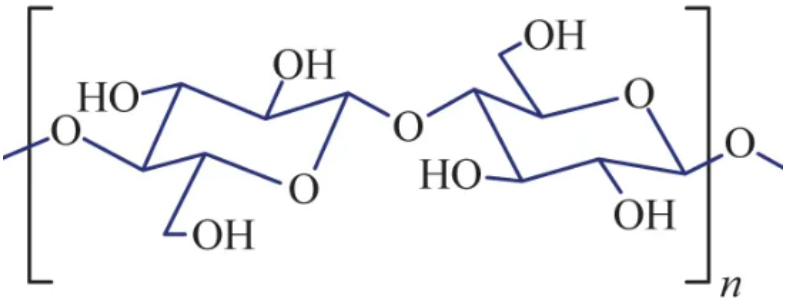

Figure 2.2: Chemical structure of cellulose.

The quantities of these components are different in each plant as shown in Table 2.3 [10].

Table 2.3: Chemical composition of some natural fibres [10].

Fibre	Cellulose (wt%)	Lignin (wt%)	Hemicellulose (wt%)	Wax (wt%)
Flax	71.0	2.2	18.6-20.6	1.7
Hemp	70.2-74.4	3.7-5.7	18.6-20.6	1.7
Jute	61.0–71.5	12.0–13.0	13.6–20.4	0.5
Kenaf	31.0–39.0	15.0–19.0	21.5	—
Ramie	68.6–76.2	0.6–0.7	13.1–16.7	0.3

Each plant fibre possesses distinct mechanical properties determined by its chemical composition. Among natural fibres, Flax is widely employed as reinforcement in structural composites due to its high cellulose content and a high degree of crystallinity, which grant its superior mechanical properties.

Structure of flax fibres

The mechanical properties are also determined by the fibre's morphological structure, which can be analyzed on three different levels as shown in Figure 2.3 [15].

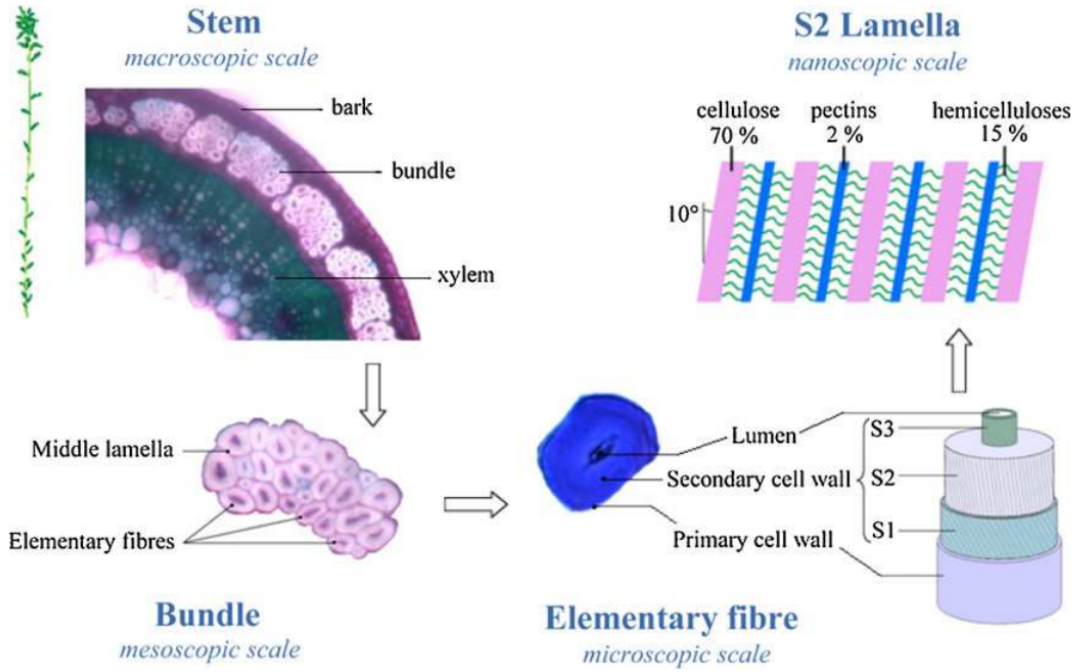

Figure 2.3: Different scale of flax fibre structure [16].

The macroscopic level is the flax stem, which is composed of concentric layers, bark, phloem, xylem and a central void, from outside to inside [15]. On a mesoscopic scale, the bundle consists of the elementary fibre and middle lamella which are bounded together by pectin [10].
At the microscopic scale, the elementary fibre is formed of two concentric cell walls, the primary and the secondary, and a central lumen. The primary wall has a thickness of 0.2 μm and envelops the thicker secondary cell wall, which, in turn, encloses the lumen that facilitates water uptake, as depicted in Figure 2.4. The secondary cell wall consists of three layers: S1, S2, and S3. Each layer is comprised of parallel cellulose microfibrils that form an angle with the fibre direction, known as the microfibril angle. It is noteworthy that the microfibril angle varies within the secondary cell wall. The mechanical properties of the cell wall layers are influenced by the microfibril angle. Specifically, as the microfibril angle increases, the layer becomes more ductile. Contrarily, a smaller microfibril angle results in a higher level of rigidity for the layer. Among these layers, S2 stands out as the thickest layer. It contains numerous crystalline cellulose microfibrils and amorphous hemicellulose, contributing to the fibre's tensile strength. The microfibril angle reaches its minimum value within the S2 layer, approximately 10° (see Fig 2.4). Consequently, S2 is considered the stiffest layer [15].
At the nano-scale, the amorphous matrix, primarily consisting of pectins and

hemicelluloses, embeds the microfibrils, which are constituted of cellulose chains. The cellulose chains within the microfibrils form crystalline zones [17].

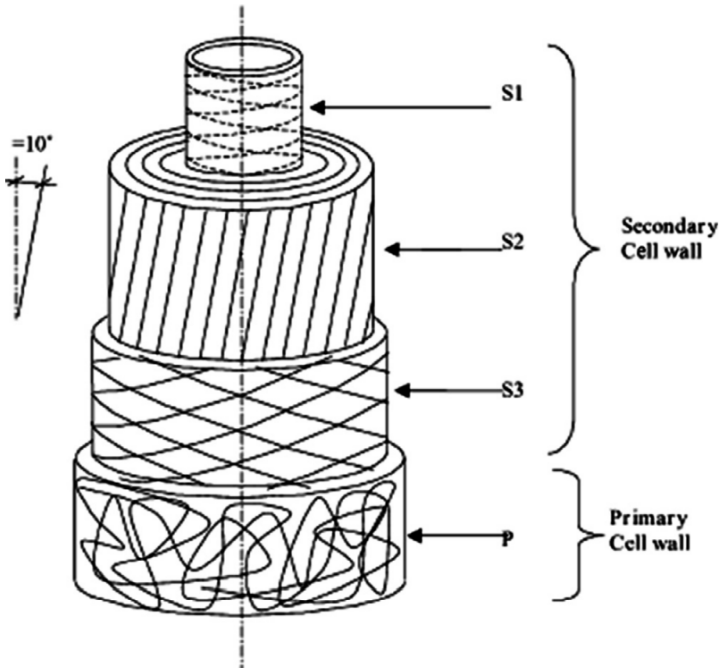

Figure 2.4: The micro-structure of a flax fibre cell [15].

Manufacturing Process

Extraction of fibre is the process in which the fibres are separated from cementing substances such as pectin or lignin, wax, resin, fats, and other carbohydrates [16]. This process can influence the mechanical properties and it is achieved in different steps:

1. **Retting**, pectins and other cells surrounding the fibre are broken down with the aid of aerobic bacteria (dew-retting) or water (water getting) [18].
2. **Scutching**, mechanical separation eliminates the bark and the xylem and separates roughly the bundles of fibres [17].
3. **Hacking**, splitting and straightening of the flax fibres, as well as further remotion of the fibrous core and further impurities [19].
4. **Chemical and physical treatments** are used to increase the cohesion between polymeric matrix and fibre in the composite or to enhance the mechanical or thermal property of the fibre without changing its chemical composition [18].

The final product is the technical fibres with the elementary fibre packaged together inside as shown in Figure 2.5.

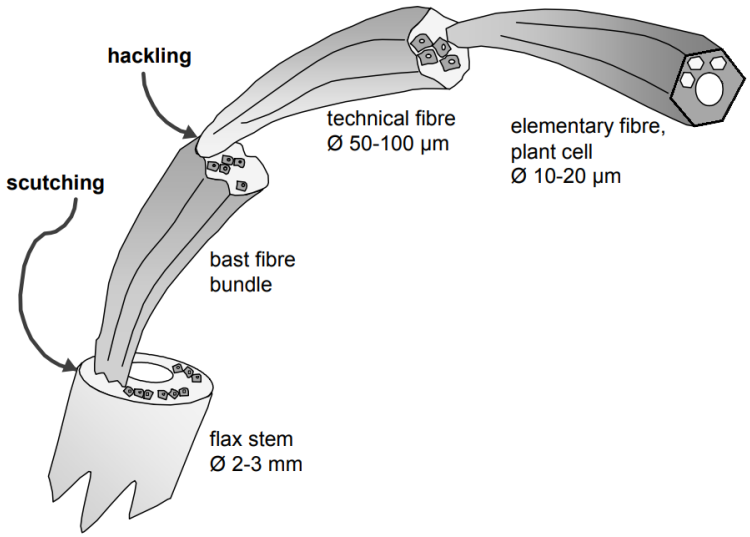

Figure 2.5: From steam to fibre [20].

Properties of flax fibre

The cross-section of elementary fibres has a polygonal shape with 7-5 sides, as shown in Figure 2.6. This characteristic facilitates the packing of the fibres together [3].

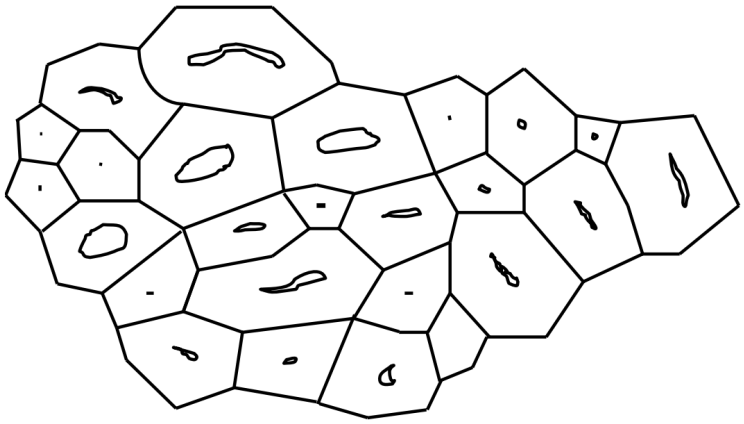

Figure 2.6: Cross section of the elementary fibre [14].

As mentioned above, cellulose and hemicellulose are the main constituents of flax fibre, being hydrophilic polymers, they also render the flax fibres hydrophilic. Therefore, their mechanical properties change with the amount of water absorbed: the strength increases and the young modulus decreases with the increasing amount of water intake. This occurs because water molecules settle not only in the lumen (central void) but also in the pores and amorphous zones of the fibre, reducing the interfibrillar cohesion and relieving the internal fibre stress [14].
Another drawback of flax fibre is its inhomogeneous quality. The mechanical properties of flax fibres are influenced by various factors, including their location within the stem, the variety of the plant, and the cultivation environment. Notably, the fibres extracted from the middle of the stem exhibit the highest strength and modulus. This is attributed to the fact that the middle part of the stem grows under more favourable weather conditions compared to the top and bottom parts [17].
Considering the physical properties of flax fibre, which are very similar to those of glass fibres, with Young's modulus of about 60 GPa and a tensile strength of 1400 MPa. This similarity makes them an environmentally friendly and lighter (with a density of around 1.45 g/cm^3) alternative to glass fibres in engineering composites. However, it is not possible to use flax fibres in applications where temperatures exceed 220°C because they start degrading [21].

2.2.2 Cellulose nanofibrils fibres

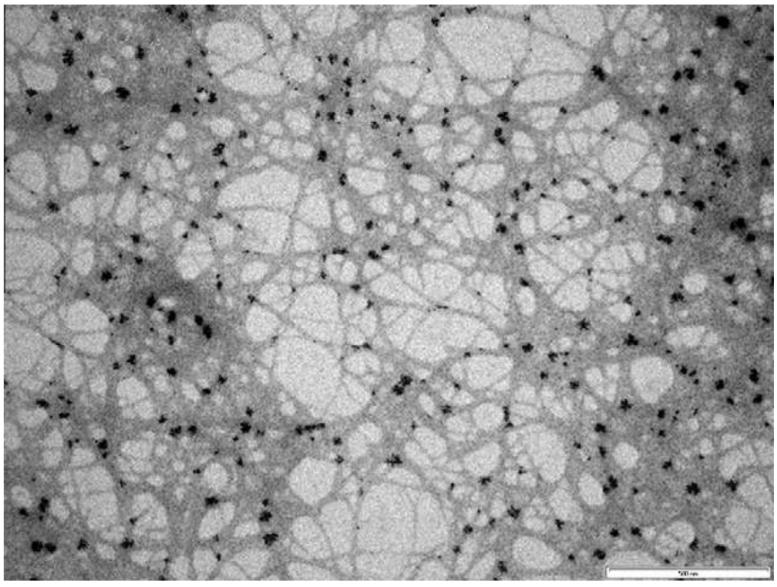

Figure 2.7: Transmission electron microscopy of CNF [22].

Cellulose nanofibrils (CNF), see Figure 2.7, are cellulose-based materials with diameters ranging from 5 to 50 nm and lengths that can reach several microns. They are extracted from wood or plants through mechanical and chemical treatments. At the end of the extraction, the nanofibrils of cellulose present both crystalline and amorphous regions due to the high shearing forces developed during this process [23]. The CNF constitute the building blocks for structural cellulose fibres. Within these fibres, fibrils are arranged in a nanoscale lamellar structure that is oriented along the fibre direction (similar to the S2 layer of natural fibre). The mechanical properties of cellulose fibres rely on the orientation of fibrils, which is controlled through the manufacturing process [5].

Manufacturing process of CNF

Cellulose is combined with hemicellulose and lignin in wood or plants. The first step in the extraction process is the remotion of non-cellulose components. Then, CNF are extracted from cellulose pulps through mechanical methods [24]. The homogenization and grinding are the most commonly used mechanical methods for CNF extraction. Homogenization applies high pressure to mechanically break down cellulose fibres into CNF. This process can be carried out using two types of machines: a homogenizer or a microfluidizer. In the case of a homogenizer, the cellulose slurry is forced through a narrow gap between the homogenizing valve and an impact ring. This action subjects the fibres to shear and impact forces, resulting in cellulose fibrillation. On the other hand, in a microfluidizer, cellulose suspensions are pushed through a thin chamber with a specific geometry, such as a Z- or Y-shape, which has an orifice width of 100-400 μm. During the passing, cellulose slurry impacts against the wall creating the shear forces, which are responsible for cellulose fibrillation. In the grinding method, the cellulose slurry is compelled to pass between static and rotating grinding disks. The shearing forces generated between the discs cause the delamination of the cell wall, leading to the individualization of nanofibrils [4]. Figure 2.8 illustrates the schematics of these mechanical treatments.
The mechanical process requires a high energy level to function, so chemical or enzymatic pretreatments of the pulps are carried out to reduce this energy requirement. Among these methods, the most effective ones are Enzymatic hydrolysis, Carboxylation via TEMPO, and Quaternization. In Enzymatic hydrolysis, enzymes are utilized to catalyze the hydrolysis of cellulose, which facilitates its fibrillation. This treatment reduces the degree of polymerization and increases the degree of crystallinity. During Carboxylation via TEMPO-mediated oxidation, the 2,2,6,6-tetramethylpiperidine-N-oxyl (TEMPO) oxidizes cellulose and facilitates mechanical disintegration. Throughout the oxidation process, negative charges are positioned into the pulp to enhance the delamination of the nanofibrils through

electrostatic repulsion. Quaternization is a process that involves cationizing cellulose by depositing quaternary ammonium cations onto the surface of nanofibrils. This creates an electrostatic repulsion force between the deposited positive ions, which in turn facilitates the process of pulp disintegration [4].

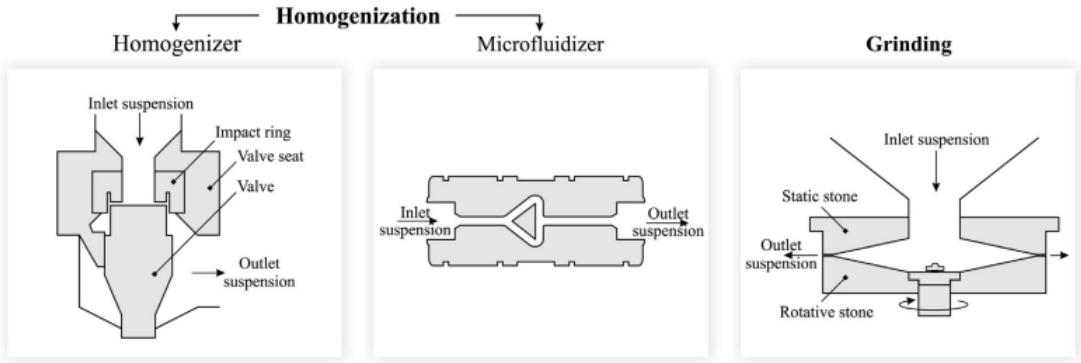

Figure 2.8: Schematics of homogenization and grinding [4].

From Nanofibrils to fibres

The hydrodynamic alignment assembles the nanostructured CNF into a macroscale fibre by controlling the surface charges of the CNF. In this process, the CNF are aligned in suspension before "locking" the nanostructure into a metastable colloidal glass. The process takes place in a double flow-focusing channel, where the assembly process takes place as shown in Figure 2.9. In the core flow (position 1), the CNF are subjected to the Brownian forces of the fluid and the electrostatic repulsion due to the presence of dissociated COOH group on their surfaces. The first sheath flow of deionized (DI) water is introduced into the main flow, which supports electrostatic repulsion and aligns the fibrils toward the flow direction (position 2). Furthermore, it encapsulates the CNF dispersion and removes it from being in contact with the channel walls. The second inserted sheath flow protonates carboxyl (COO-) groups on the surface of the CNF due to its low pH. This reduces the electrostatic repulsion between the fibrils and allows CNF to form a network transitioning the dispersion from liquid to gel thread (position 4). In the end, the continuous threads obtained are subsequently anchored at their ends and dried with air. In summary, the Flow-assisted assembly method succeeded in the assimilation of CNF into macroscale dense fibre, maximizing the efficiency of stress transfer between CNF and reducing the occurrence of stochastic defects [7].

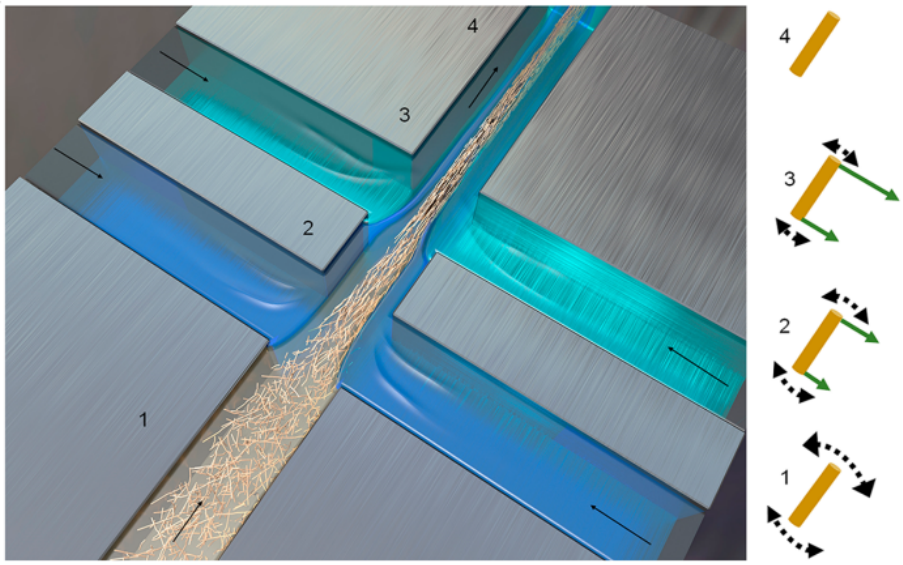

Figure 2.9: Schematic of the double flow-focusing channel used for CNF assembly. The core flow is represented as a light brown colour, DI water in a blue colour, and acid at low pH in a light green colour. The black arrow shows the flow direction. The forces acting on the CNF are illustrated on the right [7].

Fibres properties

The cellulose fibres obtained from the flow-based assembly have a density of about 1.5 g/cm^3 and a typical diameter of around $5 - 25\mu m$. The mechanical property changes according to the length of the longer CNF result in a higher degree of alignment and therefore lead to higher fibre tensile properties (Table 2.4 and Figure 2.10a). These properties are relatively independent of fibril surface charge. Furthermore, the mechanical properties are directly related to the orientation of the nanofibrils in the fibre, and they depend on the amount of absorbed water. Water indeed plasticizes the fibre, extending its plastic deformation, reducing stiffness, and increasing strain, as depicted in Figure 2.10b. Indeed, at lower humidity conditions, around 14 % RH, CNF-550 fibre reaches Young's modulus of 82 $\pm$ 4 GPa and tensile strength of 1320 $\pm$ 85 MPa. A cross-linking agent can be used to counteract the plasticizing effect of water and, consequently, increase the strength up to 1430 MPa. The chemical cross-linking maximizes the stress-transfer efficiency by creating covalent bonds between the fibrils in the fibre structure [7].

Table 2.4: Young's modulus and ultimate strength of different fibres [7].

Fibre name	Fibril length (nm)	Young's modulus (GPa)	Ultimate strength (MPa)
CNF-550	590	70	1200
CNF-820	630	70	1200
CNF-1369	391	45	630

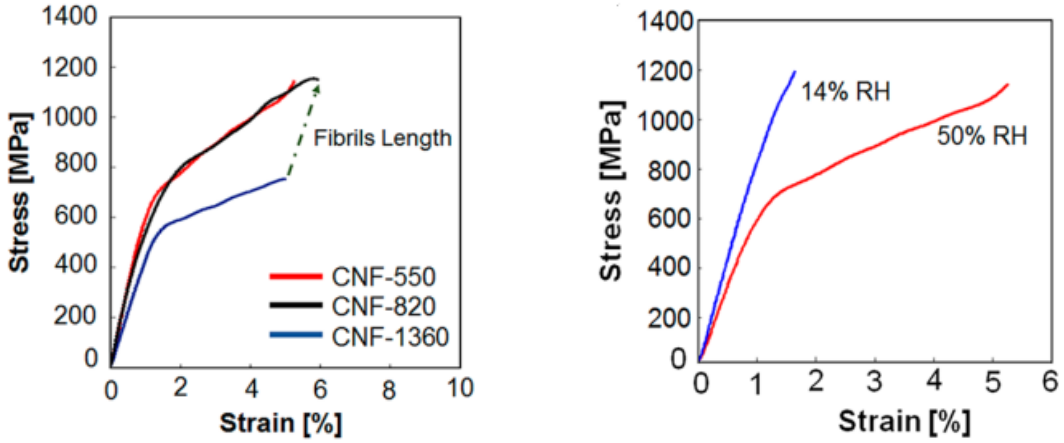

(a) (b)

Figure 2.10: (a) Stress-strain curve for CNF Fibre made of cellulose fibrils with different lengths. (b) the effect of humidity in the mechanical properties of fibre constituted of CNF-550 [7].

2.2.3 Glass fibres

Glass fibres are produced by extruding silica (SiO_2) and other oxides through tiny holes. The advantages of glass fibres include their high strength, good tolerance for elevated temperatures and corrosive environments, and low price. On the other hand, the disadvantages include moisture sensitivity, abrasiveness and difficulty in recycling, as is the case with every inorganic fibre. Different glass fibre compositions are available, with one of the most common being E ("electrical") due to its lower price, excellent electrical properties, and high durability [9].

2.2.4 Carbon fibres

Carbon fibres have a diameter of about 5 to 10 micrometres and are composed mostly of carbon atoms. They are manufactured from rayon, polyacrylonitrile

(PAN), and petroleum pitch by melting or spinning the solution. Carbon fibre is considered the stiffest and straightest reinforcement for composite materials. In addition to their high mechanical properties, they have great tolerance for corrosive environments and high temperatures, as well as low thermal expansion. On the other hand, the main disadvantages of carbon fibre are its high price, high energy consumption during the manufacturing process, brittleness, conductivity, and difficulty in recycling [9].

2.3 Hydrophilia in composite

The interface area, the contact surface between fibres and matrix, plays an important role in the mechanical properties of composite materials, as it significantly affects their strength. It transfers the load from the matrix to reinforcement, so good cohesion provides a higher strength [25]. The more chemically similar the constituents are, the stronger the bond formed between them becomes. Among the chemical characteristics, hydrophilia, the ability to bond with water molecules, strongly impacts adhesion. The element which has a stronger affinity with water, are called hydrophilic, while those with a weaker are called hydrophobic. The presence of polar groups in the chemical structure increases the degree of hydrophilic, while the presence of non-polar groups reduces it because water is a polar molecule, which binds with other molecules having a similar nature [26]. Those types of functional groups are listed below.

Polar groups:

- Hydroxyl (-OH);
- Amino ($-NH_2$);
- Carbonyl (-C=O);
- Carboxyl (-COOH);
- Phosphate ($-PO_4$)

Non-polar group:

- Methyl ($-CH_3$)

As said before, cellulose fibres are hydrophilic, while thermoset matrices are hydrophobic, so a weak cohesion between them is expected.

2.4 Matrix

The matrices for composite applications should exhibit good compatibility in terms of bonding, mechanical, and thermal properties with reinforcements. Additionally, they should be easy to process and recycle. Thermoset polymers dominate as

matrices in structural composite applications due to their superior mechanical and thermal properties compared to thermoplastics. On the other hand, the latter offer satisfactory recyclability and processability since they can be melted again once cured, unlike thermosets, which begin to degrade when heated [9].

2.4.1 Vinyl Ester

Vinylester resins are produced by the esterification of an epoxy with an unsaturated acid, such as acrylic or methacrylic. This reaction is conducted to give the Vinyl Ester the fast and simple crosslinking of unsaturated polyesters and, the mechanical and thermal properties of epoxies. In fact, its strength and chemical resistance are better than those of polyester resins but not as excellent as those of epoxy resins, and it also shows finer ductility and a lower cross-linking temperature than epoxy [9]. The typical vinyl ester is based on the reaction of Bisphenol A diglycidyl (commonly abbreviated BADGE or DGEBA). The high number of methyl groups in its chemical structure, shown in Figure 2.12, imparts hydrophobic behaviour to the vinyl ester.

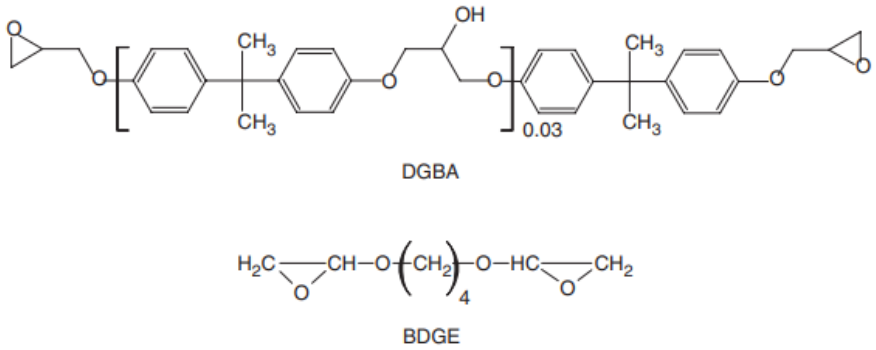

Figure 2.11: Chemical structure of Vinyl Ester [9].

2.4.2 Epoxy

Epoxy resin, also known as polyepoxides, is a thermoset polymer which contains epoxide groups. Among the thermoset resins, Epoxy has the highest mechanical and thermal properties and also it presents low viscosity, low shrinkage, and good cohesion with the reinforcement fibres. The major drawbacks of epoxies are their high prices and complex processing requirements. Indeed, many epoxies require a higher curing temperature (higher than 150°C), which can be problematic since some fibres, especially natural ones, start degrading at that temperature. Moreover, epoxy is toxic and must be handled carefully because it can create dermatitis and allergies when in contact with naked skin [9]. The presence of hydroxyl groups

in the epoxy chemical structure, see Figure 2.12, makes it more hydrophilic than Vinyl ester [27]. This ensures better cohesion with natural fibres than the Vinyl ester.

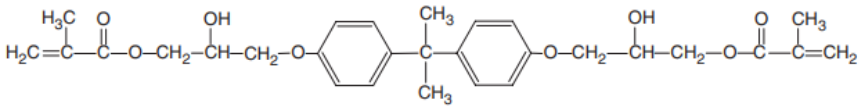

Figure 2.12: Chemical structure of Epoxy [9].

2.4.3 Polyamide

Polyamides (PAs), commonly known as nylon, are high-performance thermoplastic polymers. PAs are characterized by the presence of amine groups (-CONH-), which makes them hydrophilic and hygroscopic. This feature enables them to absorb easily water, which plasticizes them, making them less stiff and more flexible. On the benchmark, different PA grades are available, e.g., PA 6, PA 6,6 (whose chemical structure is shown in figure 2.13), and PA 12. The numbers indicate the count of carbon atoms in the repeating unit [9]. PAs exhibit good mechanical properties and excellent chemical resistance, thanks to their crystalline structure [28]. On the other hand, PAs have high melting temperatures, around 180-265°C, and low viscosity, which make the manufacturing of PA composites challenging [9].

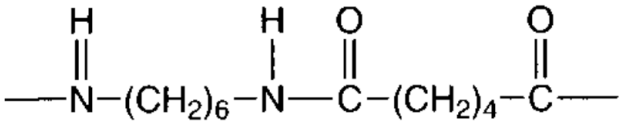

Figure 2.13: Chemical structure of PA66 [9].

2.4.4 Poly-Lactic Acid

Polylactic acid (PLA) is a thermoplastic polymer, whose repeating unit is the lactic acid (Figure 2.14), a monomer derived from renewable, organic sources such as corn starch or sugar cane. Recently, PLA has been used as a matrix in load-bearing composites instead of synthetic thermoplastic because it is fully biodegradable, non-toxic, and exhibits higher thermal and mechanical properties than those of synthetic thermoplastic polymers such as Polypropylene (PP) [29]. On the other hand, it presents some disadvantages such as low glass transition temperature, around 55°C, poor ductility, low impact strength and brittleness [30].

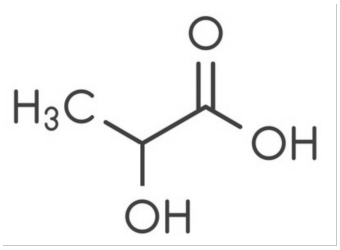

Figure 2.14: Chemical structure of lactic acid monomer.

2.5 Interface

The interface is the intermediate layer between the matrix and fibre, constituted by their bonds [31]. Its aim is to transfer the load from the matrix to the reinforcements. Thermal, mechanical, and chemical compatibility between the two composite constituents is necessary to obtain good cohesion [32]. A strong interface enables maximizing the stress transmitted from the matrix to the fibres, thereby improving the mechanical properties and thermal stability of the composite [31]. There are four fibre-matrix interfacial bonding mechanisms, which are shown in Figure 2.15:

- The **Physical adhesion** is the interdiffusion bonding mechanism based on the wettability between the two constituents. The wettability properties depend on the surface energies and polarities of fibres and matrix.
- The **Electrostatic adhesion** is the bond between opposite charges displaced on the matrix and fibre surfaces. Thus, the composite interface is formed by the interaction between anionic and cationic charges.
- The **Chemical adhesion** is the mechanism in which the interface is formed by the chemical bond between matrix and fibre such as Van der Waals and covalent bonds. It is the primary mechanism in the adhesion between organic fibre and polymer matrix composites.
- In the **Mechanical interlocking** the fibre surface is anchored to the matrix, performing like multiple hooks. A rougher fibre surface enables better adhesion.

Generally, the interfacial adhesion is a result of the multiple bonding mechanisms cited above [31].

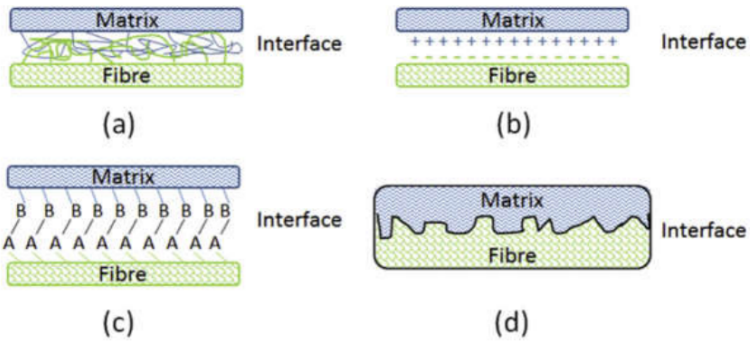

Figure 2.15: Interfacial bonding mechanisms: a) Physical adhesion; b) Electrostatic adhesion; c) Chemical adhesion; d) Mechanical interlocking [33].

The interface could be characterized by four methods: thermodynamic methods; microscopic viewing analysis; spectroscopic techniques; and micromechanical measurements [34].

2.6 Manufacturing process

The manufacturing process affects the properties of composite materials. Its aim is to maintain the reinforcement-matrix mass in the desired shape until complete solidification. Furthermore, it must completely remove the air bubbles inside the material, which could seriously reduce the mechanical properties.

2.6.1 Hot Pressing

Hot pressing is a technique for manufacturing both thermoset and thermoplastic composites since the polymers are used in the form of film and not as a liquid. Matrix films are placed above and below the laminate, and this lay-up is positioned between two half-moulds as shown in Figure 2.16. A release film is placed between the film and the half-mould to prevent the composite material from sticking to the machine. The hot mould applies heat and pressure to the gelatinous matrix, which is forced to flow through the fibre laminate and impregnate it. The resin flows perpendicular to the reinforcement laminate, driven by the pressure, which may also be higher than that of a vacuum.

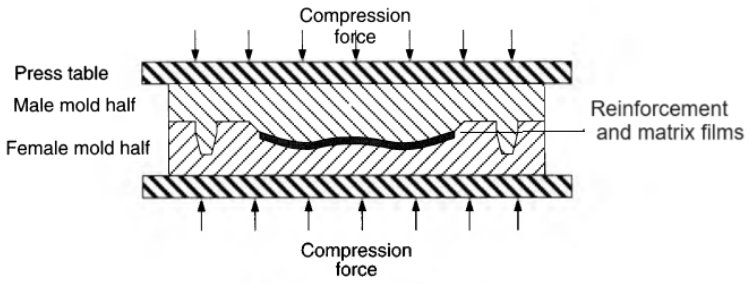

Figure 2.16: Hot pressing scheme [9].

Contrary to vacuum infusion, it is possible to choose the fibre volume ratio from the start by selecting the number of matrix layers, but on the other hand, the process is more expensive.

2.6.2 Vacuum Infusion

The Vacuum Infusion Process (VIP) is a technique used to manufacture thermoset composite materials. It is widely employed in the aerospace, nautical, and automotive fields. This process involves applying a vacuum pressure to drive liquid resin into a dry laminate, which is laid into a mould. A peel-ply is placed over the reinforcement to facilitate material removal, and a release film is placed between the laminate and the mould for the same purpose. The lay-up is sealed with a vacuum bag and tacky tape. A vacuum is applied to compact the dry materials before opening the valve and allowing the resin to flow. Once a complete vacuum is achieved, the resin is infused into the dry materials via tubes. The process ends when the resin stops flowing, and then the material is placed into the oven for post-curing of the resin. Typically, lower viscosity resins are infused because they allow for easier impregnation of the reinforcement. Sometimes a flow media is used to aid the flow and, consequently, reduce the infusion time. It is important to note that viscosity decreases during the process due to the curing of the resin. Vacuum infusion offers substantial emission reductions [35]. The vacuum infusion set-up and lay-up are illustrated in Figure 2.17

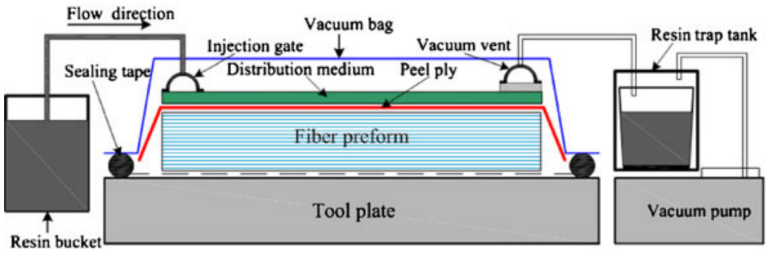

Figure 2.17: Vacuum Infusion Process scheme [36].

The main advantages of the vacuum infusion process are that the air is completely removed from the product, the material is not subject to elevated temperature and the process is relatively low in price. The main disadvantage is that it is not possible to control the amount of resin that flows into the laminate, thus making it difficult to control the fibre volume ratio [9].

2.6.3 Resin Transfer Molding

Resin Transfer Molding is a manufacturing process of thermoset matrix composite. It consists of the injection of resin into a closed mould where the dry reinforcements are placed, the schematic of RTM is depicted in Figure 2.18. A pressurized air drives resin into the mould, where it must fill all voids inside. Therefore, resin penetrates and wets all the reinforcement surfaces. In the mould, there are some vents, through which the entrapped air is removed from the resin in order to manufacture a void-free composite [9]. The main advantage of RTM is that it enables the achievement of the desired FVR by regulating the amount of injected resin and applying a high fiber compaction pressure, which can reach over 1 MPa.

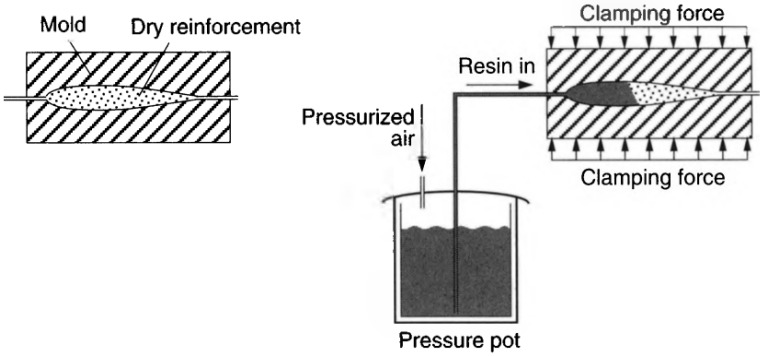

Figure 2.18: The schematic of RTM [9].

2.7 Mechanical characterization and properties of composite material

The tensile test consists of pulling the composite specimens until failure and observing how they respond by evaluating the following parameters:

- Young's moduli E_l and E_t;
- Poisson's ratios ν_{lt} and ν_{tl};
- Tensile strengths, σ_l and σ_t;
- Ultimate tensile strains, ϵ_l and ϵ_t.

The letters "t" and "l" indicate the longitudinal and transverse directions to the fibres, respectively. Rectangular specimens are used for the test and tabs are added at the ends, as depicted in Figure 2.19, to reinforce those parts, as the clamping force of the tensile machine acts on them. The test is only valid if the specimen fails in the middle.

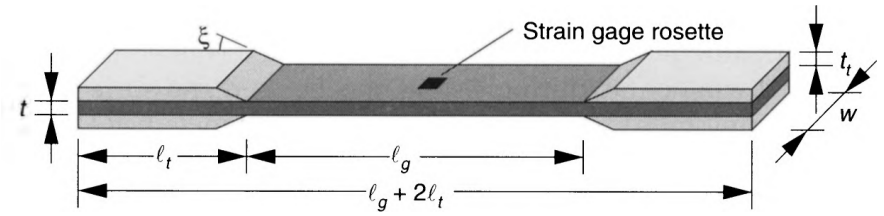

Figure 2.19: Common geometry of tensile test specimen, l_g is the useful length, t is the thickness of composite and t_t thickness of tabs [9].

The tensile test could be performed by applying a constant rate of strain ($d\epsilon/dt$) or displacement speed between the two ends, which is called a control displacement test. This method allows for the calculation of ultimate tensile strain, unlike the control displacement load method, which applies the increase of load over time (dF/dt) [37]. During testing, a load cell senses the applied load, while the strain gauges sense the elongation. The results of the test are the curve of load vs. displacement, and then the graph of stress vs. strain is computed from the geometry of the specimen, an example is given in Figure 2.20.

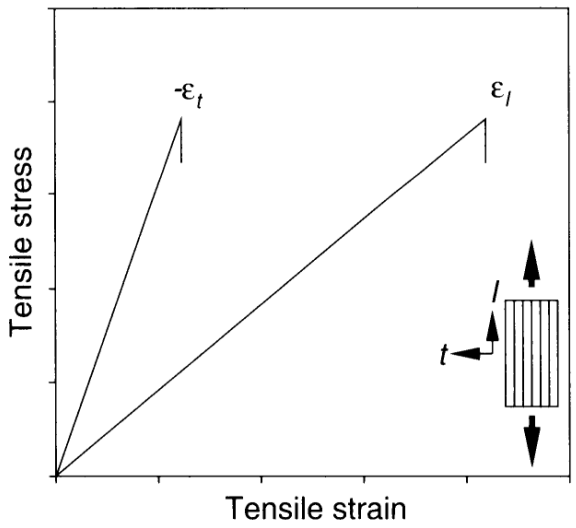

Figure 2.20: Example of stress-strain relationships for tensile testing [9].

The young modulus is the slope of the graph while the Poison's ratio is the ratio between the strain in the two perpendicular directions:

$$\nu_{lt} = -\frac{\epsilon_t}{\epsilon_l} \qquad \nu_{tl} = -\frac{\epsilon_l}{\epsilon_t} \tag{2.1}$$

Ultimate tensile strength and strain represent the stress and deformation at the point of fracture.

2.7.1 Failure modes

When a UD composite laminate is pulled along the fibre longitudinal direction, the reinforcements primarily bear the tensile load. The possible failure modes of one layer Unidirectional composite plate in the tensile test are:

- **Fiber-matrix debonding** begins with the formation of cracks at the interface between the matrix and fibres. These fractures then propagate along the fibre direction until they completely break the specimen, causing the fibres to be pulled out of the matrix. This failure mode occurs when the cohesion between the matrix and reinforcement is too weak.
- **Fibre fracture** occurs when the fibres are the first to break, and the cracks propagate until the composite undergoes complete failure.

- **Matrix cracking** starts, as the word itself suggests, with a crack into the matrix and then runs parallel to the fibre until the plate fails. This failure mode is most common during the tensile test in the transverse direction.

These three failure modes can occur simultaneously or separately depending on the shear resistance of the fibre, matrix and interface [32]. The failure modes are illustrated in the below picture:

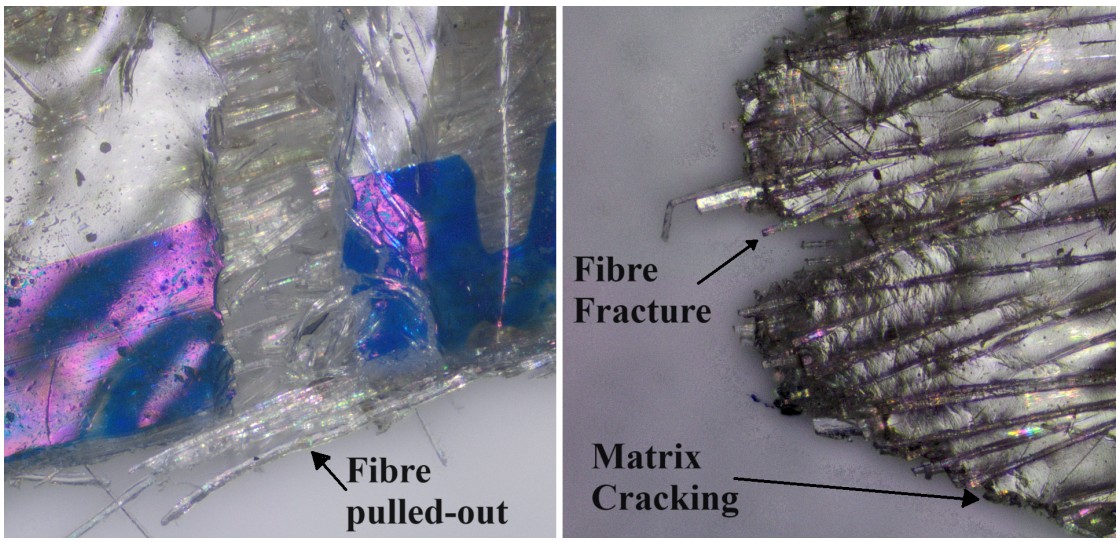

Figure 2.21: Failure mode of composites during the tensile test.

Chapter 3

Method and Material

3.1 Material

This section presents details on the types of fibres, cellulose and flax, and matrices, epoxy and vinyl ester, employed in composite manufacturing.

3.1.1 Fibres

CELLUXTREME provides two CelluloseNanoFibrils fibre plates shown in Figure 3.1 and their physical properties are presented in Table 3.1.

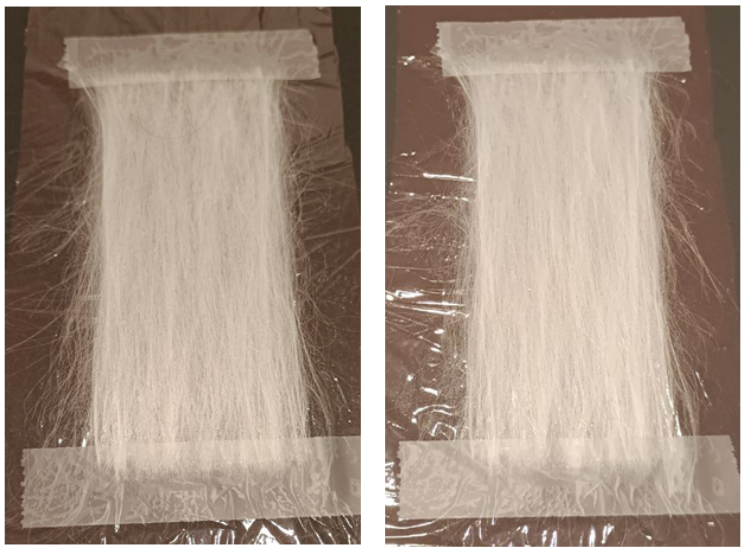

Figure 3.1: First and second CNF plates, respectively on left and right.

As the production process of CNF is under development, the mechanical properties of cellulose fibres are not optimized, so the expected Young's modulus is not yet as high as the maximum found in the literature (70 GPa).

Table 3.1: CNF Fibre physical properties.

	Size (cm x cm)	Areal weight (g/m^2)	mass (g)	density (g/cm^3)
1°	5x10	78	0.38	1.5
2°	5x10	76	0.36	1.5

The utilized flax fibres are the AmpliTex-Art. No. 5057 supplied by Bcomp, as shown in Figure 3.2, whose physical and mechanical properties are:

- Areal weight measured in ambient with 22 °C and 50 % RH: 150 g/m^2;
- Thickness plate: 0.41 mm;
- Fibre density: 1.47±0.02 g/cm^3;
- Elongation at break: 1.3-1.4%;
- Apparent Modulus: 63±1 GPa [38].

Figure 3.2: AmpliTex-Art. No. 5057.

3.1.2 Matrices

The first plate will be impregnated with an epoxy film in the hot pressing, whereas the second plate will undergo vacuum infusion with vinyl ester.
HexPly 6376 is a high-performance tough epoxy film formulated for the fabrication of primary aircraft structures. Its Curing conditions are:

- 2 hours at 175°C and 7 bar of pressure;
- Heat up rate from 2°C to 5°C [39].

DION 9100 Bisphenol-A Epoxy-based vinyl ester Resin has good corrosion resistance and high strength. The properties of the two matrices are written in Table 3.2.

Table 3.2: Matrices physical and mechanical properties.

Property	HexPly 6376 [39]	DION 9100 [40]
Tensile Modulus (GPa)	3.60	3.17
Tensile Strength (MPa)	105	80
Elongation at Yield (%)	3.1	5.2
Density (g/cm^3)	1.31	1.13
Viscosity (cps)	–	500

The matrices are selected primarily for their high mechanical properties, rendering them suitable for load-bearing applications. Additionally, the aim is to investigate how organic fibres interact with two matrices having different levels of hydrophobia in two manufacturing processes, hot pressing and vacuum infusion.

3.2 Method

Processing cellulose fibre is very challenging for two main reasons: the thin nature of the plates and its incompatibility with hydrophobic matrices. Many trials have been conducted using thin carbon and flax fibre to address these two issues. This chapter presents the final configuration of the manufacturing processes for cellulose fibres. Additionally, identical processes are applied to flax fibres, and the results are compared in terms of cohesion with matrices and mechanical properties.

3.2.1 Hot pressing

The first step is to dry the fibre plates by placing them in the oven (Beschickung-Loading Modell 100-800) for 60 minutes at 60°C, as indicated in the flax datasheet [38], in order to remove the moisture content, which could affect the cohesion with

the matrices [32]. After that, the material is prepared for the hot pressing process, which is made up of three steps:

1. **Consolidation**, the material is placed into the oven for 2 h at 90°C under full vacuum pressure, in that way the resin is forced to flow into the reinforcement and impregnate it without curing.

2. **Heating**, the impregnated fibres are heated from room temperature (25°C) to the curing temperature (175°C) for 1 hour, with a heating rate of around 3.5°C per minute. During the heating process, the pressure is maintained at 7 bar.

3. **Curing**, a pressure of 7 bar is applied, and the material is kept at 175°C for 2 hours until fully cured.

The lay-up for consolidation is illustrated in Figure 3.3. For cellulose fibre, the epoxy films are placed over and under it. For flax fibre, due to the greater thickness, four matrix layers are required, with two for each side: top and bottom. The breather is necessary to distribute even pressure. The cork frame surrounds the laminate plate and the sucker, as shown in Figure 3.4, distributing pressure from the centre to the exterior due to the frame's greater height compared to the composite thickness. This pressure distribution allows for the complete removal of air from the fibre plate through the suction action of a vacuum pump. The lay-up is completely sealed with a vacuum bag and tacky tape. The temperature is chosen to minimize epoxy viscosity. However, lower pressure might not succeed in fully impregnating the fibres and removing air bubbles.

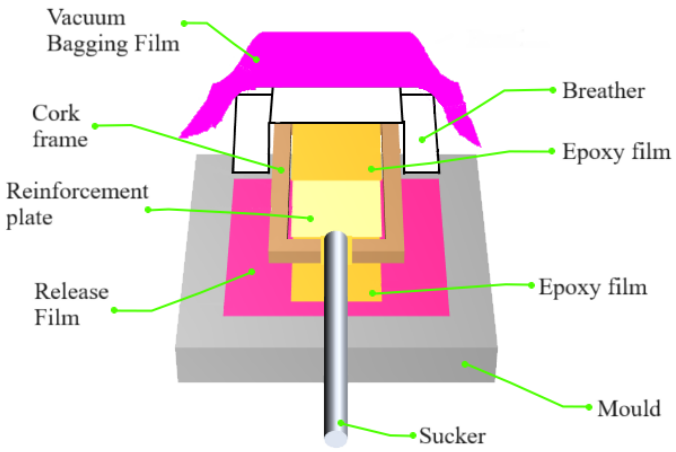

Figure 3.3: Consolidation lay-up.

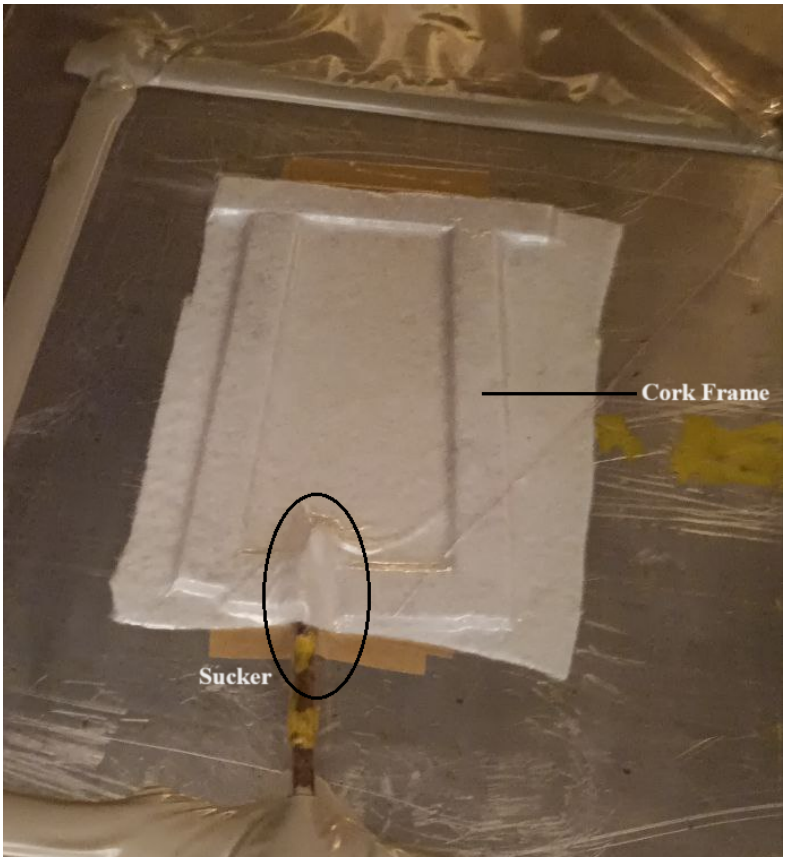

Figure 3.4: Consolidation set-up.

After the consolidation, the impregnated material is taken out from the bag and set in Fontune Presses, a hot-pressing machine, for curing. The minimum load (15 kN) exerted by the machine is too high for the small surface area (5x10 cm) of the specimen to achieve the required pressure of 7 bar ($p = \frac{15[kN]}{10x5[cm^2]} = 30[bar]$). Therefore, a rubber sheet (25x25 cm) is used to distribute the force over a larger area, thus to apply the correct pressure ($p = \frac{44[kN]}{25x25[cm^2]} = 7.04[bar]$), scheme in Figure 3.5. Figure 3.6 illustrates the changes in temperature, depicted in blue, and pressure, depicted in red, during the heating and curing process.
The Fontune Presses has the following features:

- load range of 15-600 kN;
- maximum press force of 22.5 MPa;
- maximum Temperature of 300 °C.

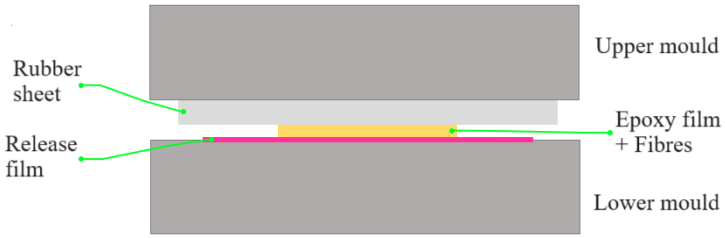

Figure 3.5: Hot pressing set-up.

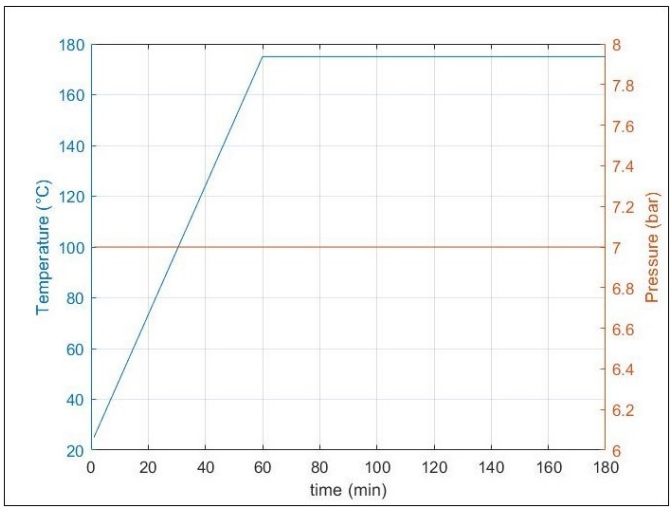

Figure 3.6: Trend of temperature, in blue, and pressure, in red, in hot pressing Machine

3.2.2 Vacuum infusion

After the drying of the reinforcement plate, as done for the other one (heat it in the oven for 60 minutes at 60°C), it is sealed in a vacuum bag following the layup indicated in Figures 3.7 and then a vacuum is applied to compact the material and remove the air inside. Figure 3.8 displays the vacuum infusion set-up before the resin injection. Various release perforated films have been tried between the peel ply and reinforcement plate. Still, they have yielded unsatisfactory results because they either slowed the flow or stuck to the fibre. Therefore, none of them has been decided to be used. The distribution weaves over the peel ply are not employed, as they could also increase the roughness of the composite's upper surface.

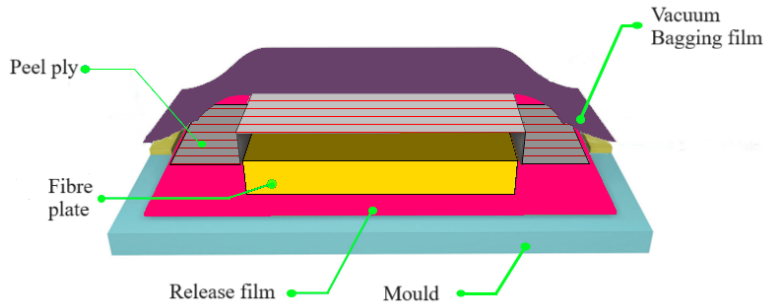

Figure 3.7: Vacuum infusion lay-up.

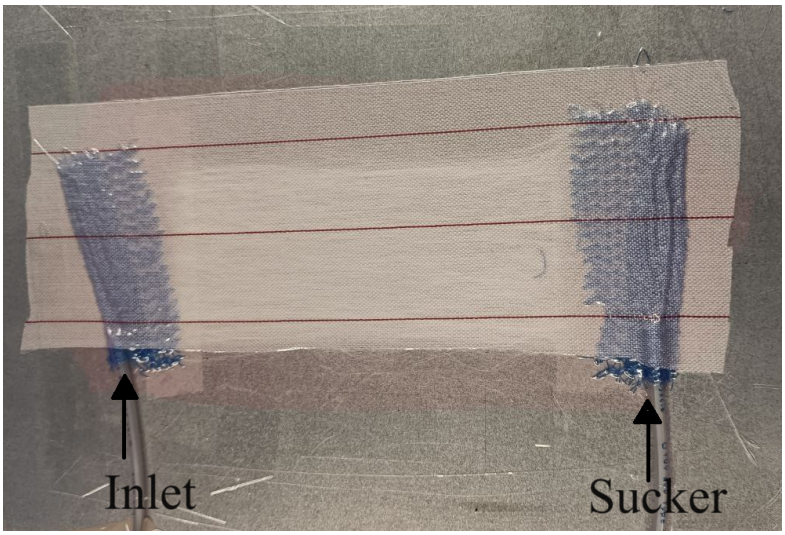

Figure 3.8: Vacuum infusion set-up.

The distribution weaves are rolled up around the inlet and sucker (both have the same internal diameter of around 2.22 mm) to linearize the resin flux, see Figure 3.9. The vinyl ester must be mixed with the initiator to start the curing process, as well as with an accelerator and inhibitor to control the gelation time, which has to be longer than the infusion time. The mixture has been chosen to obtain a gelation time of around 45 min, the receipt is indicated by Table 3.3.

Table 3.3: Curing system.

Component	Name	Percentage (%)	Weight (g)
Resin	Dion 9100	100	50
Accelerator	Acc. 9802 (Cobalt 1%)	3	1.5
Inhibitor	Inh 9853 (TBC 10%)	0.5	0.25
Initiator	Butanox LTP	2	1

After mixing, the resin is left to degas for 10 minutes to remove any air bubbles that have formed during the mixing process. Then, the resin is injected into the fibre under a pressure of 0.7 bar, rather than using the full vacuum (1 bar). This is because if the full vacuum were applied, the shear stress at the top and bottom of the laminate would be too high, which could slow the flow down as explained in Appendix A. When resin reaches the sucker the valve pressure is opened more to reduce the pressure to 0.4 bar for the further stabilization of the flow. The process concludes when the resin reaches a state of stillness. After that, the material, still sealed in the vacuum bag, is heated in the oven from room temperature (25°C) to 60°C, and then this temperature is maintained for 6 hours. Once the resin has cured, the composite is slowly cooled down to room temperature. This is the post-curing process, which is necessary to accelerate the curing process and optimize the final properties of the composites [41].

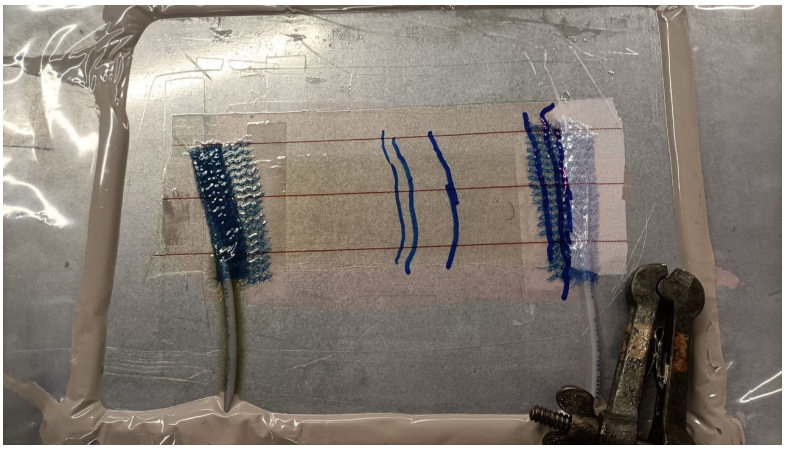

Figure 3.9: Resin flow in vacuum infusion, the blue lines are markers of the flow front.

3.3 Microscopy

Once the vinyl ester and epoxy have cured, the following steps are taken to prepare the edges for microscopy: they are cut perpendicular to the fibre direction, clamped, and embedded within the VariDur 200 matrix. The surfaces to be observed are polished using a Vector Power Head grinder, following the steps indicated in Table 3.4. The Olympus BX50 microscope is utilized for examining the cross-section and analyzing the adhesion. Figure 3.10 pictures specimens prepared for microscopy.

Table 3.4: Grinding process

Step	Surface	Abrasive/Size	Load $[kN]$	Base speed $[rpm]$	Time $[min : sec]$
1°	CarbMet	320 grit SiC	27	300	Until plane
2°	VerduTex	9 μm Liquid Diamond	27	150	5:00
3°	VerduTex	3 μm Liquid Diamond	27	150	5:00
4°	VerduTex	0.5 μm MasterPrep Alumina	27	150	1:30

Figure 3.10: Specimens ready for microscopy, CNF+VE on left and CNF+E on right.

After microscopy, the main dimensions of fibre cross-sections are measured using ImageJ, an image-processing software. For flax fibre, the width and height of the cross-section are considered, while for CNF fibre, two perpendicular diameters are taken into account.

3.4 Fibre volume fraction evaluation

The thicknesses of composite materials are directly measured using the microscope software (Olympus Stream Basic) in the captured pictures. From these images, the Fiber volume ratio (FVR) of the manufactured composite materials is evaluated using ImageJ. These results are then compared with the FVR estimated by measuring the mass of the composite (m_c) with Mettler Toledo, a scale with an accuracy of 0.0001 g, while the fibre weight (m_f) is already known:

$$m_m = m_c - m_f \tag{3.1}$$

$$V_f = m_f/\rho_f \tag{3.2}$$

$$V_m = m_m/\rho_m \tag{3.3}$$

$$FVR = \frac{V_f}{V_f + V_m} \cdot 100 \tag{3.4}$$

Where "m," "V," and "ρ" represent mass, volume, and density, respectively, while the subscripts "m" and "f" indicate that these properties correspond to the matrix and fibres, respectively.

3.5 Sample preparation

The lateral sides have lower mechanical properties due to the edge effect and the heterogeneous distribution of fibres in the plate. Indeed, the amount of fibre is higher in the middle, where they are densely packed, and lower at the sides. For this reason, those sections are cut out, and the remaining portion is divided into five samples (seven for CNF+VE only) with a width of 5 mm and a length of 50 mm, as illustrated in Figure 3.11. Five is the minimum number of specimens required for testing in order to achieve a statistically valid distribution of the results.

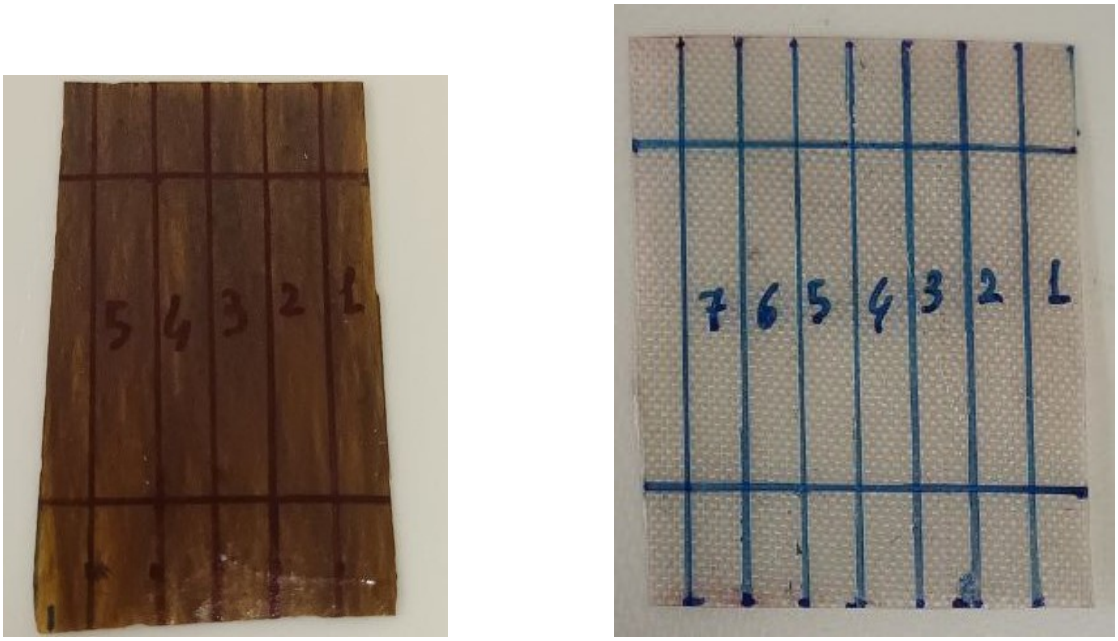

(a) CFN+E. **(b)** CFN+VE.

Figure 3.11: Division of surface and numeration of samples for testing, CFN+E on left and CNF+VE on left. The horizontal lines at the edges of samples indicate where tabs are going to be placed.

The next step is tab preparation: tabs are cut from a standard thermoset plate, and each tab must measure 10 mm in length and 15 mm in width. Four tabs are needed for each sample, with two for each end. It is not recommended to use thermoplastic tabs because they have poor adhesive properties with the glue, which could result in the composite specimen slipping out during the tensile test. Subsequently, the surfaces where the tabs will be attached are polished using sandpaper to improve cohesion with glue. The tabs are then glued by the Epoxy Adhesive 9466 Loctite, to the ends of the specimen as shown in Figure 3.12. The tab and specimen sizes are chosen to achieve an aspect ratio (gauge length: width) as close to 5:1 as possible. In this case, since the gauge length is approximately 3 cm and the width is 0.5 cm, the aspect ratio results around 6:1. Then the tabbed sample dimensions are measured with a Mitutoyo, a digital calibre with an accuracy of 0.001 mm.

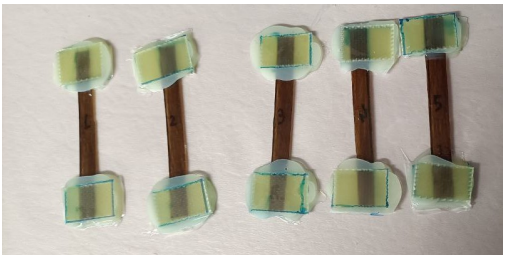

(a) CFN+E.

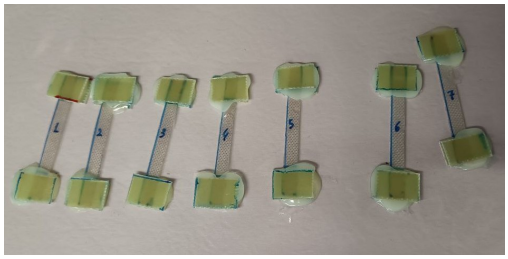

(b) CFN+VE.

Figure 3.12: Tabbed sample, CFN+E on the left and CNF+VE on the right.

3.6 Tensile test

The machine used for the tensile test is the Shimadzu AGS-X Series, with load cells of 5 kN and an accuracy of 10^{-7} N. The sample is carefully clamped between the jaws in a way that ensures vertical alignment from the upper clamp to the lower one, as Figure 3.13 shows. This alignment prevents the specimen from being subject to side loading or bending during the test. Usually, an extensometer is required to better detect the sample elongation during the test. In this case, using an extensometer is not possible due to the sample's short gauge length. Before starting the test, it is necessary to set the preload of 0 N to eliminate the presence of any preexisting axial load, which could potentially alter the test results. During the test, the specimen is slowly elongated at a speed of 0.3 mm/min. For tensile testing of composite materials, an elongation speed of 0.01 mm/min/mm is typically applied. Considering a gauge length of 30 mm, the test speed is 0.3 mm/min. Trapezium X-V, the data-gathering software, monitors the force acted upon the specimen and displays the curves for the load (F) versus displacement (ΔL). The gathered data from the tensile test are processed in Excel to calculate stress (σ) versus strain (ϵ) graphs. Stress is computed by dividing the applied load (F) by the initial sample cross-section (width "w" x thickness "t"), while strain is calculated by dividing the displacement (ΔL) by the initial gauge length of the specimen ("L_0").

$$\sigma = \frac{F}{w \cdot t} \qquad \epsilon = \frac{\Delta L}{L_0} \tag{3.5}$$

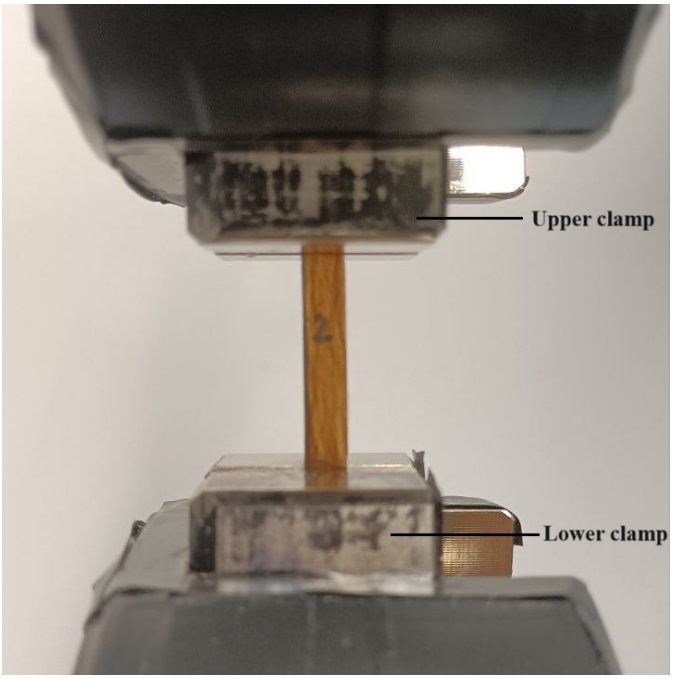

Figure 3.13: Correct configuration of tensile test.

From those graphs, the following properties are possible to evaluate:

- Young's modulus is the slope of the linear-elastic phase, given by $E = \frac{\Delta\sigma}{\Delta\epsilon}$. Points close to zero are not taken into account because non-linear phenomena may occur at the beginning of the tensile test, which can make the material appear less stiff than it actually is.
- Tensile strength σ_{max} is the maximum stress, representing the stress at which failure occurs.
- Elongation at break ϵ_{max} is the strain corresponding to the tensile strength.

3.7 Estimation of fibre stiffness

"Rule of mixture" equations are widely used to predict the stiffness of fibre-reinforced composites based on the weighted contributions from the fibre and the matrix [42]. So, given the composite stiffness (E_c) from the tensile test, the stiffness of the matrix (E_m) from the datasheet and the fibre volume ratio (FVR), which is calculated as described above, Young's modulus of the fibre can be estimated as

follows:

$$E_c = E_f \cdot FVR + E_m \cdot (1 - FVR) \tag{3.6}$$

$$E_f = \frac{E_c - E_m \cdot (1 - FVR))}{FVR} \tag{3.7}$$

One of the assumptions of this model is that the fibres must be aligned in one direction. However, this assumption is not valid because not every cellulose fibre is perfectly stretched in the main direction, as evident in Figure 3.1. The "Ten-percent rule" corrects Young's modulus error caused by fibre misalignment. The "Ten-percent rule" is a substantial approximation that assumes each fibre not aligned with the main direction contributes only one-tenth of the axial stiffness [43].

$$E_x = E_1 \cdot \lambda \tag{3.8}$$

$$\lambda = 0.1 + 0.9 \cdot (0°\%/100) \tag{3.9}$$

E_x represents Young's modulus of the fibre plate in the main direction, E_1 represents the stiffness of the fibre, and the parameter $(0°\%/100)$ denotes the percentage of fibre aligned in the main direction. Determining the exact value for the last parameter can be challenging; therefore, a range between 50-100 % is considered. The corrected Young's modulus is calculated by inverting Equation (3.8):

$$E_1 = E_x/\lambda \tag{3.10}$$

3.8 Theoretical and measured Young's modulus

The measured Young's modulus of the four composite plates is compared with the theoretical values evaluated using the Rule of mixture, as defined by Equation (3.6). The stiffness values for flax fibre and matrices are sourced from their respective datasheets [38], [39], [40]. Regarding CNF fibre, the considered stiffness value is the evaluated one.

3.9 Adhesion study

After failure, the broken zones are observed under a microscope to understand which failure mode has occurred, providing information about the matrix-fibre adhesion.

Chapter 4

Results

4.1 Manufacturing

Figure 4.1 shows the appearance of cellulose-fibre composites manufactured by hot pressing with epoxy film on the left and by vacuum infusion with vinyl ester on the right.

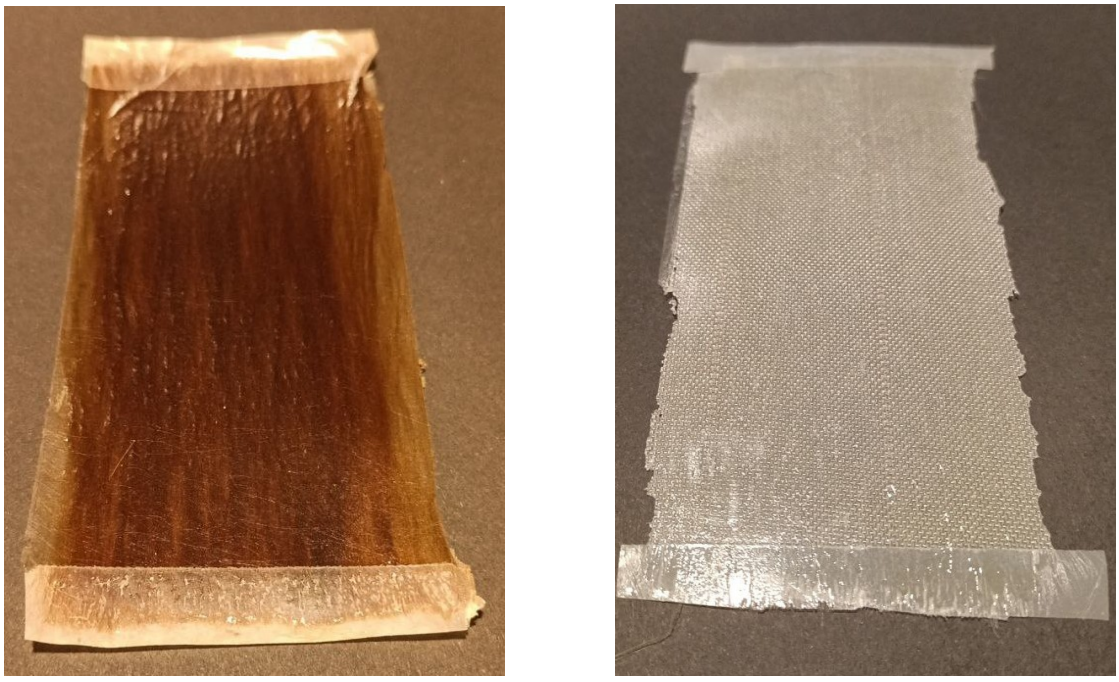

(a) CNF+E. **(b)** CNF+VE.

Figure 4.1: Manufactured CNF+E on left and CNF+VE on right.

4.2 Microscopy

Figure 4.2 and 4.5 show how CelloseNanoFibrilis' and Flax's fibres adhere respectively to Epoxy and Vinyl Ester.

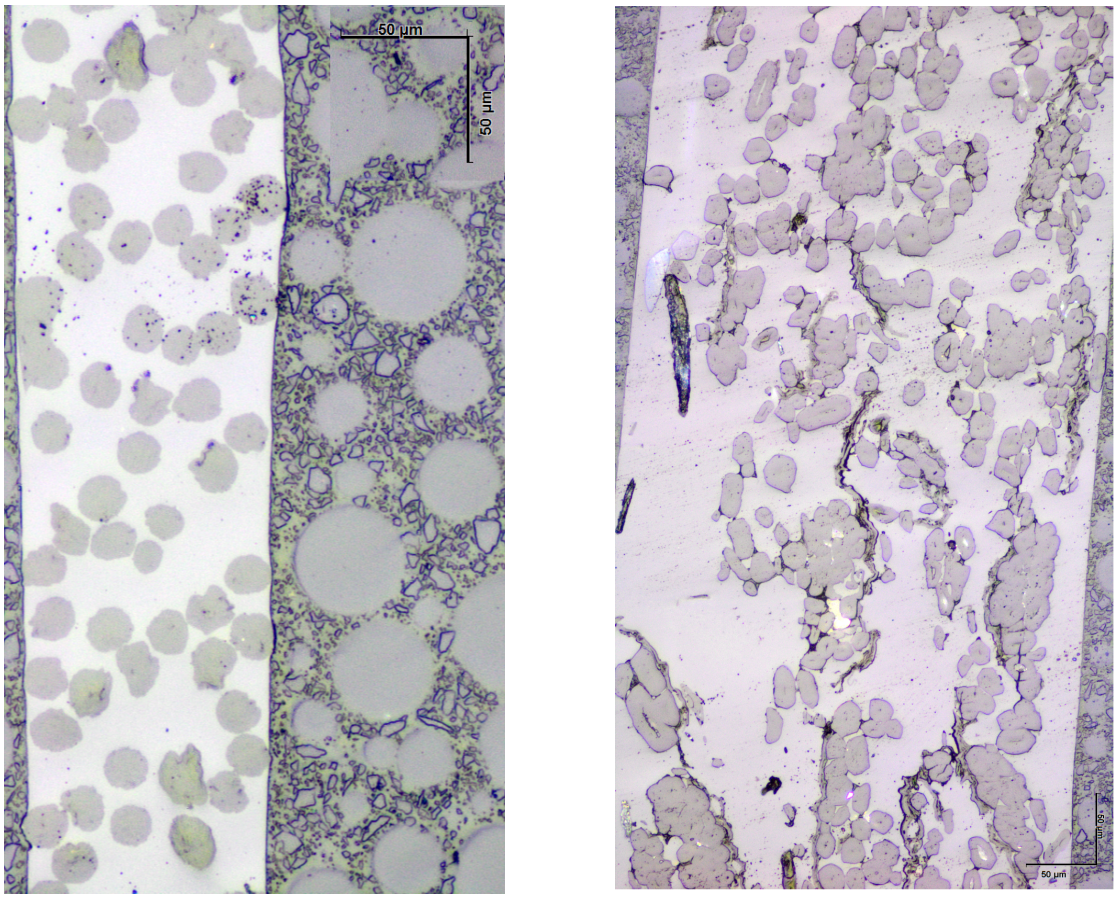

(a) CNF+E. **(b)** Flax+E.

Figure 4.2: Cross-section of CNF+E on left and Flax+E on right.

Figure 4.3 and 4.4 depict the impact of the cork frame during the consolidation phase of hot pressing, showing respectively the cross-section and the side view.

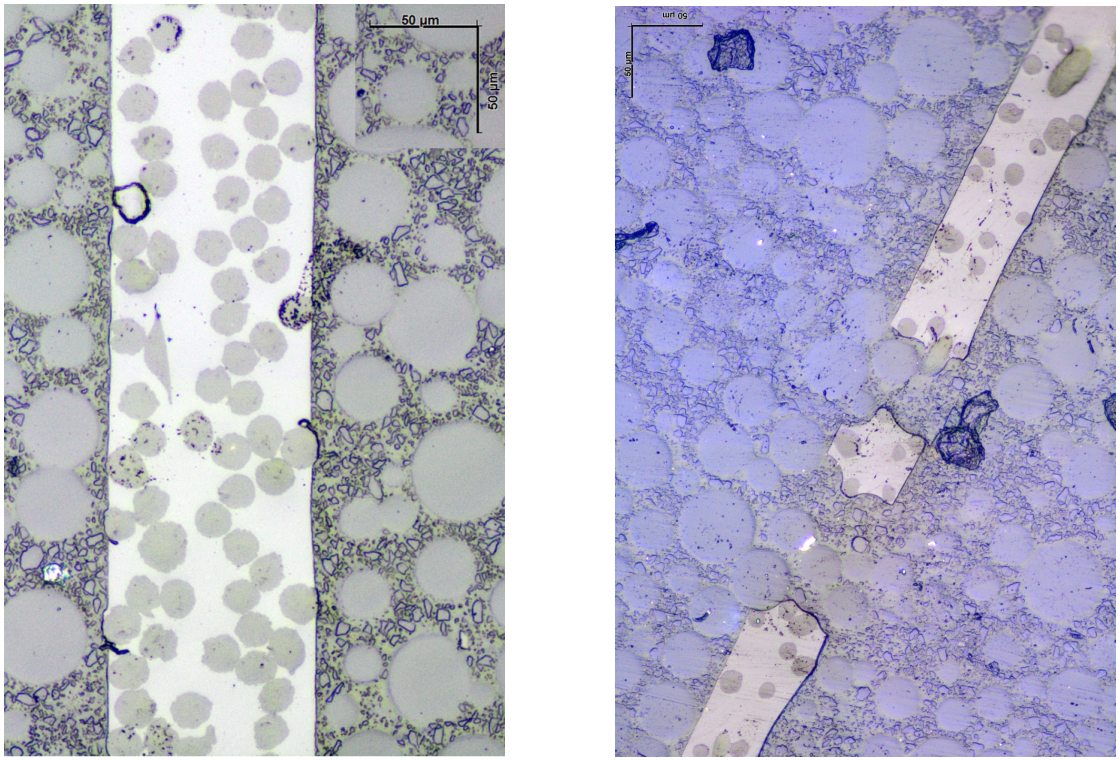

(a) With cork frame.

(b) Without cork frame.

Figure 4.3: Cross-section of CNF+E consolidated with the cork frame on the left and without the cork frame on the right.

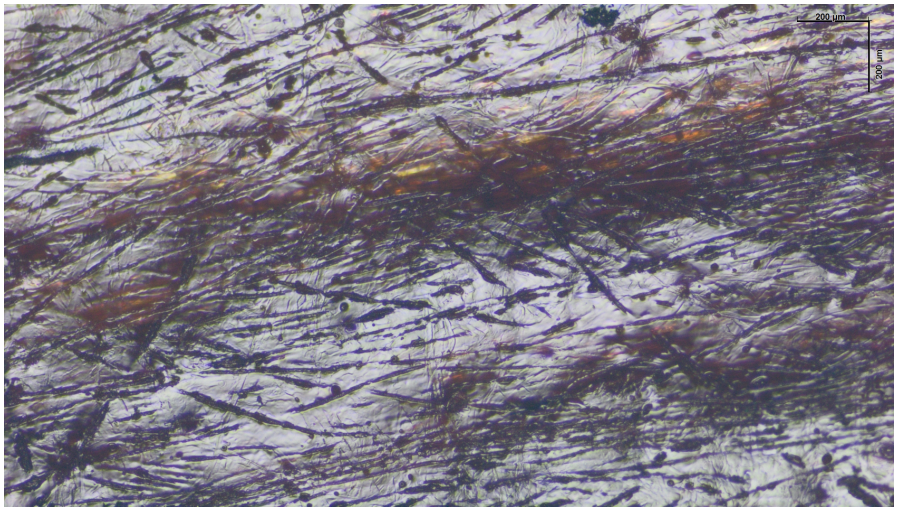

(a) With cork frame.

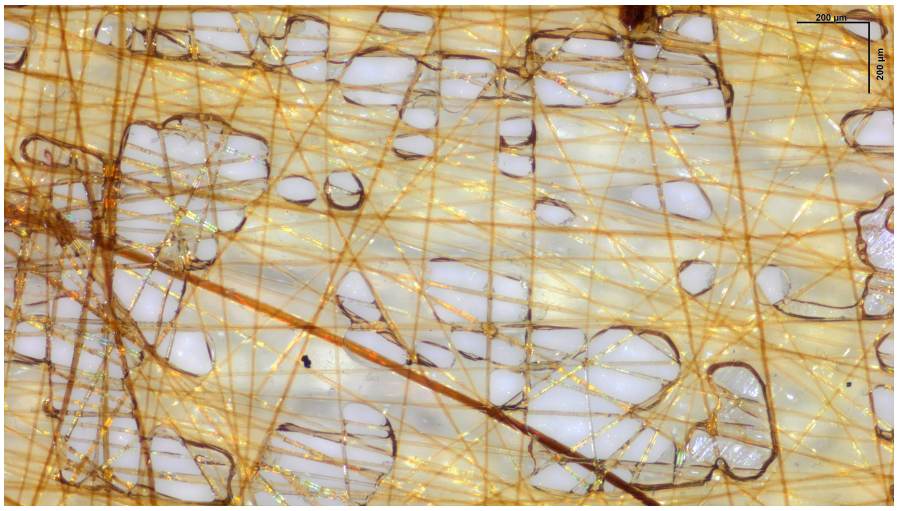

(b) Without cork frame.

Figure 4.4: The side views of CNF+E are shown, consolidated with the cork frame on the top and without the cork frame on the bottom.

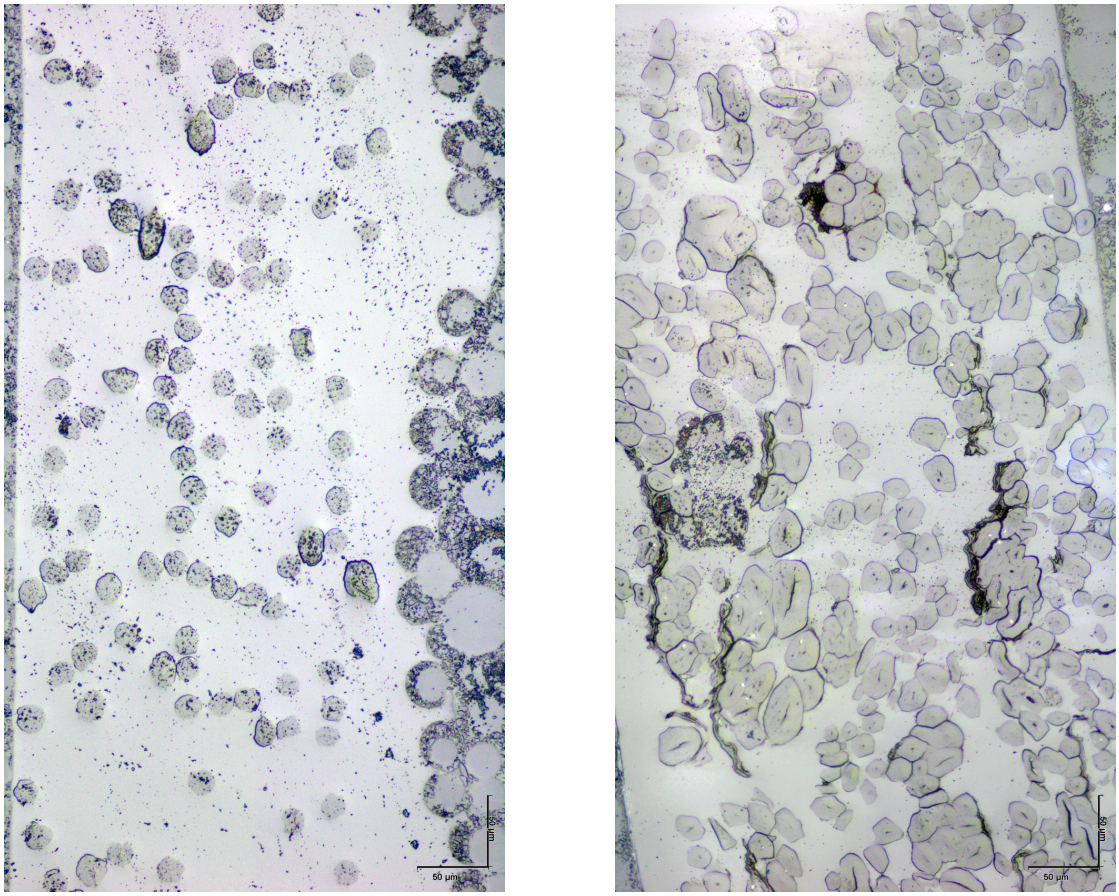

(a) CNF+VE. **(b)** Flax+VE.

Figure 4.5: Cross-section of CNF+VE, on left and Flax+VE on right.

Table 4.1 provides data about the geometry and sizes of cross-sections of two types of fibres, including their standard deviation. Which dimensions are measured and their values are documented in Appendix B.

Table 4.1: Shape and dimensions of fibre cross-sections.

Fibre	Shape	First mean direction (μm)	Second mean direction (μm)
CNF	Circle	19.5 ± 2.3	17.5 ± 1.9
Flax	Polygon with 5 to 7 sides	20.5 ± 4.1	13.4 ± 2.5

4.3 Thickness and fibre volume ratio evaluation

Table 4.2 provides the data about the evaluated thickness and fibre volume ratio of manufactured composite plates. The mean thickness is calculated as the average of the various measurements taken along the cross-section, reported in Appendix C, excluding the side parts. This exclusion accounts for the edge effects that reduce the thickness of the material at the side.

Table 4.2: Thickness and fibre volume ratio of composites.

Fibre	Matrix	Process	Mean thickness (μm)	FVR (%)
CNF	Epoxy	Hot pressing	105	≈ 50
CNF	Vinyl Ester	Vacuum infusion	282	≈ 18
Flax	Epoxy	Hot pressing	285	≈ 50
Flax	Vinyl Ester	Vacuum infusion	510	≈ 28

4.4 Sample dimension

The following tables provide information about the tested sample sizes for each manufactured composite.

Table 4.3: Sample dimension of CNF+E.

	Gauge length (mm)	Width (mm)	Thickness (mm)
1°	25.00	4.92	0.1
2°	26.16	5.11	0.1
3°	22.72	5.11	0.1
4°	25.56	4.95	0.1
5°	27.32	5.52	0.1

Table 4.4: Sample dimension of CNF+VE.

	Gauge length (mm)	Width (mm)	Thickness (mm)
1°	27.82	5.30	0.28
2°	25.98	5.39	0.28
3°	28.32	5.00	0.28
4°	26.21	4.88	0.28
5°	27.95	5.03	0.28
6°	27.10	5.17	0.28
7°	27.71	5.57	0.28

Table 4.5: Sample dimension of Flax+E.

	Gauge length (mm)	Width (mm)	Thickness (mm)
1°	26.95	4.18	0.26
2°	26.46	5.11	0.23
3°	26.44	4.96	0.24
4°	28.16	4.86	0.26
5°	28.16	4.88	0.29

Table 4.6: Sample dimension of Flax+VE.

	Gauge length (mm)	Width (mm)	Thickness (mm)
1°	28.57	4.85	0.49
2°	29.77	5.77	0.54
3°	27.23	4.77	0.49
4°	28.54	5.15	0.44
5°	25.85	4.82	0.49

4.5 Theoretical and measured Young's modulus

Table 4.7 provides information on the proximity of the measured Young's modulus to the theoretical value for each type of manufactured composite plate. Appendix D contains the evaluated values of mechanical properties, including Young's Moduli, for four tested composites, as well as Young's Modulus of CNF fibres used in the calculation of the theoretical Young's Modulus.

Table 4.7: The percentage ratio between the measured and theoretical Young's modulus of four manufactured composites.

Composite plate	Measured/ Theoretical Young's modulus	Fibre volume ratio
CNF+Epoxy	80 %	$\approx 50\%$
Flax+Epoxy	56 %	$\approx 50\%$
CNF+Vinyl Ester	65 %	$\approx 18\%$
Flax+Vinyl Ester	48 %	$\approx 28\%$

4.6 Fibre-matrix adhesion

Figure 4.6 illustrates the failure modes for the four composite materials at the end of the tensile test.

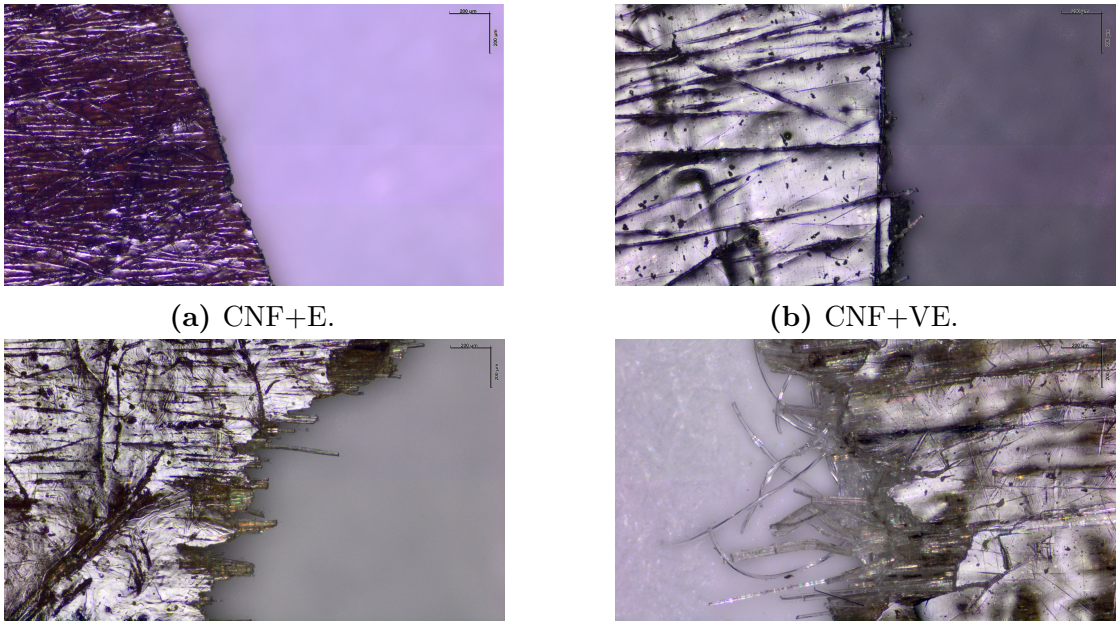

(a) CNF+E. **(b)** CNF+VE.

(c) Flax+E. **(d)** Flax+VE.

Figure 4.6: Failure modes for the different tested composite.

Chapter 5

Discussion of the results

5.1 Manufacturing

The virgin fibres in Figure 3.1 do not exhibit any significant colour in their appearance, so they can be considered transparent. The two plates exhibit a chromatic difference after manufacturing, as shown in Figure 4.1. Indeed, the first fibre plate, processed at a high temperature (175°C), appears darker than it did in its unprocessed state. Meanwhile, the second plate, heated at 60°C for 6 hours, maintains its initial appearance. It is highly likely that the temperature to which the cellulose fibres were exposed during the hot pressing caused either the fibres to burn out or some chemical reaction with air.

5.2 Microscopy

Figure 4.5 shows that the composite plate has surfaces with different roughness: the bottom is completely smooth because it was in contact with the mould during the infusion, while the top has a roughness of approximately 20 μm since the peel ply left its imprint on it.
The cork frame is essential in the consolidation, as it succeeds in removing completely the air bubbles inside the fibre plates, allowing adequate impregnation. Its absence results in an incorrect pressure distribution, starting from the exterior and progressing toward the centre of the plate. This led to air bubbles becoming trapped in the middle of the plate, as shown in Figures 4.3 and 4.4, with no air bubbles visible near the edges.
The difference in geometry between the two types of fibres, flax and CNF, is evident under microscopy. Indeed, cellulose fibres have a circular shape, with a regular size of approximately 19 μm in diameter, as observed in Figures 4.2a and 4.5a and detailed in Table 4.1. Some fibres appear to have a more elongated cross-section

than others because they are not aligned in the main direction, so they have not been cut perpendicularly to their axis. On the other hand, flax fibres exhibit a polygonal shape with sides ranging from 5 to 7. Figures 4.2b and 4.5b illustrate their irregular geometry, as both size and shape vary widely from one fibre to another. Additionally, the distribution of fibres is not as homogeneous as that of CNF fibres; some fibres are more densely packed together while others are isolated. The dimension irregularities are outlined in Table 4.1, which details that the standard deviation of flax fibre's longest dimension is double that of CNF's diameter. Furthermore, flax fibres feature a circular void in the middle, known as the lumen, which is absent in CNF fibres. CNF fibre regularity is due to their manufacturing process (Flow-assisted assembly method), which gives them the homogeneous quality as explained in the Theoretical background chapter.
As explained in the Method section, the observation of the composite cross-section provides information about the bonding between matrix and fibre. The composite constituents adhere perfectly if there are no defects in their interface. Blue lines and scratches are some possible defects in the interface, which represent respectively a poor cohesion between fibre and matrix and a complete detachment. The formation of the blue line could be due to the presence of small voids between fibre and matrix, which are subsequentially filled during the pouring of the VariDur 200, the blue matrix utilized in the sample preparation for the microscopy. While the scratches denote a repulsion between the two phases. There are a lot of interface scrapes in the cross-section of flax fibre composite material; on the contrary, they are completely absent in the CNF fibre composite, as depicted in Figures 4.5 and 4.2. Therefore, the thermoset matrices bind more effectively with cellulose fibre than flax ones. Taking into account only the cellulose composite cross-section, the number of blue lines is greater in the vinyl ester matrix composite than in the epoxy one. This confirms what was established in paper [27]: epoxy create stronger bonds with hydrophilic fibres than vinyl ester, thanks to the high number of hydroxyl groups in the chemical structure. These settlements are further demonstrated by analysing the failure modes of composites in the tensile test.

5.3 Thickness and Fibre volume ratio evaluation

The hot pressing process achieves the desired fibre volume ratio, which is between 50 and 55 %, as the amount of resin is chosen ahead of schedule as explained in the Theoretical background chapter. On the contrary, this is not possible by the vacuum infusion, due to a limitation regarding the maximum applied force for material compaction, which is the vacuum (101 325 Pa). So, it results in a fibre volume ratio approximately of 18 % for cellulose fibre composite and around 28 % for flax fibre composite. This difference is due to the different packaging

of reinforcement plates: flax fibres are more efficiently aligned and packed more densely than CNF fibre.

5.4 Theoretical and measured Young's modulus

The measured Young's modulus of the cellulose-based composite could not reach the value of theoretical ones due to imperfect cohesion among the two components of the composites. The stiffness of CNF+E (80%) is closer to the theoretical value than CNF+VE (65%) because epoxy has a higher degree of hydrophilicity than Vinyl Ester, allowing it to bind better with hydrophilic fibres. Additionally, fibre misalignment is another aspect that influences the impossibility of reaching the ideal value, since the fibres oriented in a different direction than the primary ones do not contribute completely to the axial stiffness of composites. Furthermore, it has been observed that fibres with altered colour have almost doubled Young's modulus compared to fibres treated at a lower temperature; this phenomenon can affect the difference in the percentage ratio between cellulose-epoxy and cellulose-vinyl ester composites.
The flax fibres are perfectly aligned in the main direction, so the lower percentage ratios between the real and ideal composite stiffness, 56% for flax-epoxy and 48% flax-vinyl ester composites, are caused by the poor adhesion between hydrophobic matrices and hydrophilic fibres. Another reason may be that the value of Young's modulus indicated in the datasheet (64 GPa) [38], and used for the calculation of the ideal Young's modulus, might not correspond to the real value.

5.5 Adhesion study

The most common failure mode of the studied flax fibre composite is fibre pull-out, whereas the studied CNF fibre composites fail homogeneously, which means that the failure is due to fibre fracture and matrix cracking with no or, at least, small damage at the interface. In the former case, the failure also occurs at the interface, which indicates poor cohesion between the flax fibre and the thermoset matrix. This is more evident in the Vinyl Ester-Flax composite due to a larger number of debonded fibres than in the Epoxy-Flax composite, as depicted in Figure 4.6. In conclusion, CNF fibres are shown to have more potential in load-bearing applications thanks to their good compatibility with thermosets matrices. Further discussion about the calculated mechanical properties of manufactured composites and their comparison is contained in Appendix F.

Chapter 6

Conclusion

This thesis work aimed to manufacture a composite plate with a fibre volume ratio suitable for structural applications (ranging from 50% to 55%). This goal was achieved in the epoxy-based composite processed via hot pressing. The studies of the interphase between the fibre and matrix through microscopy and analysis of the failure zone revealed that CNF fibres demonstrated greater potential in load-bearing applications compared to flax fibres, owing to their better compatibility with thermoset matrices. This was particularly evident in the epoxy-based composite, as it exhibited superior binding with hydrophilic fibres compared to Vinyl Ester, confirming findings from the literature review. These results represent an advancement towards the utilization of cellulose fibre as a valid substitute for synthetic ones, aiming to reduce emissions during the production of fibres for structural composite materials.

6.1 Future development

To enhance the mechanical properties of the composites, the primary recommendations are to Improve the stiffness of the fibres and their orientation within the plate. Increasing the percentage of the fibre oriented in the main direction facilitates the matrix flow in the fibre reinforcement both in the fibre direction (vacuum infusion) and in the direction perpendicular to the plate (hot pressing), as well as improves the longitudinal mechanical properties of composite material.
The work conducted in the paper [7], produced CNF fibre with elevated mechanical properties: 70 GPa of Young's modulus and 1320 MPa of Tensile strength. If these fibres were used, the composites manufactured in this work would have the

following mechanical properties: [1]

$$E_{CNF+E} = 36.80\text{GPa} \qquad \sigma_{CNF+E} = 712.50\text{MPa}$$
$$E_{CNF+VE} = 15.20\text{GPa} \qquad \sigma_{CNF+VE} = 303.20\text{MPa}$$

Both processes have room for improvement. In hot pressing, the elevated curing temperature exposes cellulose fibres to physical or chemical reactions, altering their chromatic and mechanical properties. To address this, a future modification could involve maintaining the vacuum during the curing of epoxy to prevent fibre chemical reactions with the air. Additionally, the use of an epoxy with a curing temperature below 120°C is necessary to prevent such fibre reactions. This temperature limit is estimated based on preliminary studies of cellulose fibre behaviour conducted in Appendix G.
On the other hand, the performed vacuum infusion did not succeed in achieving the desired fibre volume ratio. Therefore, it is necessary to increase the compaction pressure to squeeze out the excess resin and pack the fibre more densely. Unfortunately, this value is limited in vacuum infusion. Therefore, possible solutions include applying further pressure on the fibre plate or completely changing the manufacturing process by implementing Resin Transfer Molding (RTM).
Another possible future development is to strengthen the matrix-fibres cohesion by executing chemical pre-treatment. For example, a coupling agent is used to enhance chemical bonding. The coupling agent is a bifunctional molecule with one end forming a bound with a compatible group of fibres, and the other end reacting with the compatible group of the matrix. Silane (SiH_2) is a conventional agent used for natural fibre composite because it has a hydrophilic end which binds with the hydrophilic group of fibre and a hydrophobic end which reacts with hydrophobic groups in the matrix. Alternatively, Maleated can be used as well [33].
The manufactured composites in this work are partially biodegradable, as they contain both bio-fibers and thermoset matrices. The importance of using fully biodegradable green composites is becoming increasingly significant. Therefore, a further step could be the fabrication of a completely environmentally friendly composite by replacing the thermoset matrices with bio-based alternatives. Another way to enhance the recyclability properties of composite plates is by replacing the thermoset matrix with a thermoplastic matrix, as thermoplastics can be recycled more easily. Among the thermoplastic polymers, Poly-lactic acid (PLA) and Polyamide (PA) are expected to adhere efficiently to cellulose fibres due to their hydrophilic behaviour. Combining PLA, which has already demonstrated better

[1] Those properties are estimated by using the "Rule of Mixture" and considering the FVR of manufactured composite, 50% for CNF+E and 18 % for CNF+VE.

compatibility with natural fibres than Polypropylene [29], with CNF fibres results in a fully biodegradable composite material.

Appendix A

Flow in composite manufacturing process

The resin flow in the composite during the vacuum infusion is described by the continuity equation A.1 and the equation of motion A.2:

$$\frac{\partial \rho}{\partial t} + \nabla \cdot (\rho U) = 0 \tag{A.1}$$

$$\rho \frac{DU}{Dt} = -\nabla P + \nabla \cdot \tau \tag{A.2}$$

Where:

- ρ is the density;
- U is the velocity vector;
- τ is the viscous stress tensor.

The relationship between the viscous stress tensor, τ and the rate of strain tensor γ', and consequently, the definition of strain tensor are necessary to complete the equation set:

$$\dot{\gamma}_{i,j} = (u_{i,j} + u_{j,i}) \tag{A.3}$$

$$\tau_{ij} = -\frac{2}{3}\mu(\nabla \cdot U)\delta_{ij} + \mu\dot{\gamma}_{i,j} \tag{A.4}$$

where, μ is the viscosity and δ_{ij} is the Kronecker factor. The previous equations are valid if the density and viscosity are constant during the resin flow [44]. Truthfully, they change during the infusion, but they can be considered constants because their evolution is very slow. The solution of this equation system is the velocity

vector, which has a parabolic profile in a plane parallel to the fibre as illustrated in Figure A.1: it reaches the maximum value in the middle of channel height and is 0 in contact with the edges. As equation A.4 explains the shear stress is a function of the velocity gradient and it reaches its maximum value at the edges. If the height channel is too low, velocity changes more rapidly over the high, resulting in a very high shear stress, which could slow the flow down.

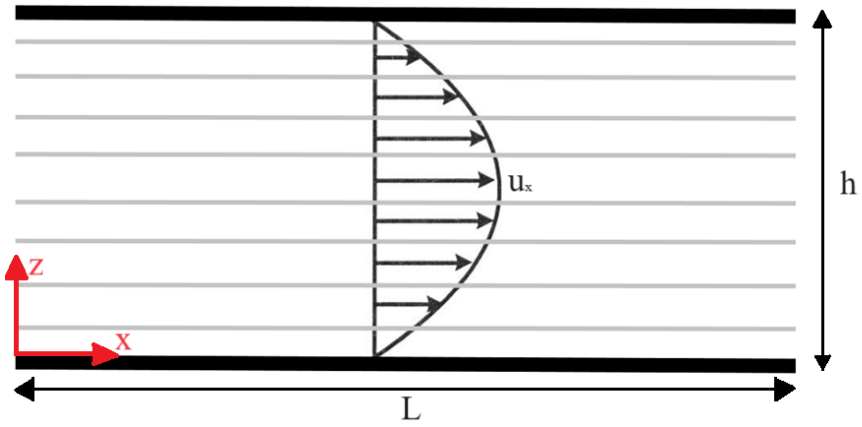

Figure A.1: Velocity profile of the resin flow in the reinforcement plate.

Appendix B

Measurements of cross-sectional dimensions

The cross-sectional shapes of fibres are approximated to an ellipse for CNF fibres, where the longest axis is indicated with d_1 and the shortest axis with d_2, and to a polygon with 5 to 7 sides for flax fibres, where the longest dimension is indicated with w and the shortest with h, as illustrated in Figure B.1.

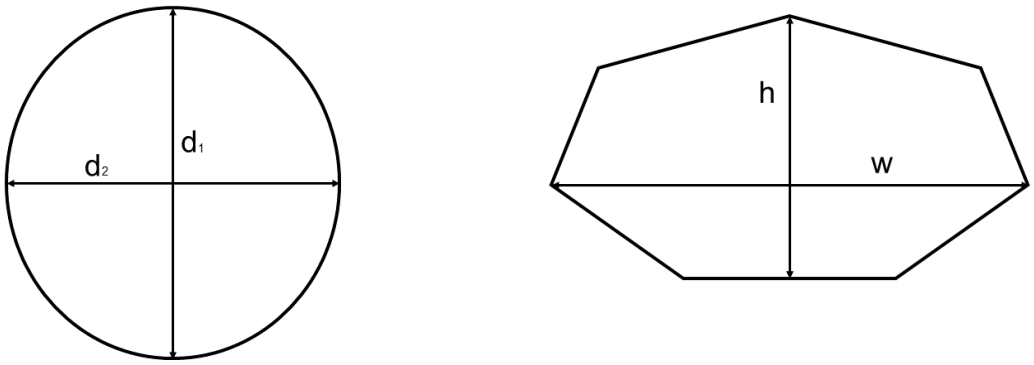

(a) CNF. **(b)** Flax.

Figure B.1: Approximated scheme of cross-sections of CNF fibre on left and flax fibre on right.

Tables from B.1 to B.4 provide the measurements of the main dimensions of the cross-sectional area of CNF and flax fibres, including their mean values and

standard deviations in μm.

Table B.1: Measured longest diameter (d_1) of CNF fibre and its mean value.

Measured diameter d_1 (μm)				
16.4	19.1	19.2	19.1	21.7
18.3	16.9	20.9	19.2	17.5
21.6	18.6	20.1	21.0	19.8
18.6	16.2	20.4	19.1	20.0
25.2	18.8	17.6	18.1	17.6
24.7	17.8	23.5		
Mean value (μm)			19.5	
Standard Deviation (μm)			2.3	

Table B.2: Measured shortest diameter (d_2) of CNF fibre and its mean value.

Measured diameter d_2 (μm)				
15.8	16.2	16.6	16.3	19.7
14.6	16.5	18.4	17.9	17.7
16.9	17.2	17.0	17.8	18.9
16.5	20.3	18.5	18.9	16.9
19.1	17.0	18.2	19.9	15.8
17.8	16.1	22.6		
Mean value (μm)			17.5	
Standard Deviation (μm)			1.9	

Table B.3: Measured longest dimension (w) of flax fibre and its mean value.

Measured width w (μm)				
26.1	17.8	19.4	16.2	23.5
18.2	19.1	14.8	22.6	21.1
25.6	13.1	22.6	20.6	24.3
24.6	22.4	24.3	17.8	14.3
19.8	22.0	14.9	14.4	28.1
18.6	24.6	24.2		
Mean value (μm)			20.5	
Standard Deviation (μm)			4.1	

Table B.4: Measured shortest dimension (h) of flax fibre and its mean value.

Measured height h (μm)				
14.8	15.0	14.4	14.2	12.1
12.7	10.9	12.6	12.9	15.1
11.5	7.5	16.0	16.8	15.2
12.4	11.4	11.2	12.9	9.1
9.4	16.9	15.1	14.5	16.9
13.9	17.7	12.5		
Mean value (μm)			13.4	
Standard Deviation (μm)			2.5	

Appendix C

Thickness measurements

Tables C.1 and C.2 list the measurements of the thickness of the four manufactured composite plates, including their mean values.

Table C.1: Measured thickness and its mean value of CNF+E.

Measured thickness (μm)			
88.57	96.81	96.44	88.97
109.24	105	90.86	116.7
102.24	93.76	103.28	116.72
107.77	112.24	98.92	144.28
119.6	99.29	107.79	111.11
Mean value (μm)		105.48	

Table C.2: Measured thickness and its mean value of CNF+VE.

Measured thickness (μm)			
301.2	329.19	318.49	224.33
253.96	238.41	260.66	292.81
275.67	305.25	287.87	306.69
304.64	298.94	260.92	282.71
253.81	297.12		
Mean value (μm)		282.92	

Appendix D

Results of fibres and composite stiffness

Company confidential

Appendix E

Results of tensile test

Company confidential

Appendix F

Discussion about the results of fibre and composite stiffness

Company confidential

Appendix G

Preliminary studies about the thermal behaviour of CNF fibre

Studying the thermal behaviour of CNF fibres and how temperature influences their mechanical properties is important to understand the maximum limit at which fibres can be treated. A simple test was carried out to estimate the maximum temperature under which fibres do not change their chromatic and possible physical properties. This test consists of heating the waste fibres and keeping them at a specific temperature for 1 h in the oven, and after that, calculating the weight lost. The tested temperatures were 120°C, 135°C and 175°C and their effects are illustrated in Figure G.1 and G.2. The results of this quick test settle that 120°C

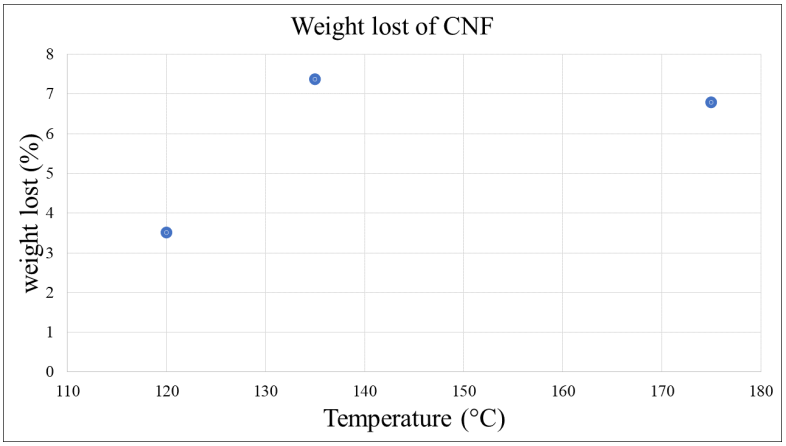

Figure G.1: Weight lost.

is the maximum temperature that did not affect the fibre colour. It is important to underline that this is only a preliminary assumption based on a very quick test. Therefore, it will be necessary to perform a more accurate test in order to determine the actual influence of temperature on CNF fibre mechanical properties.

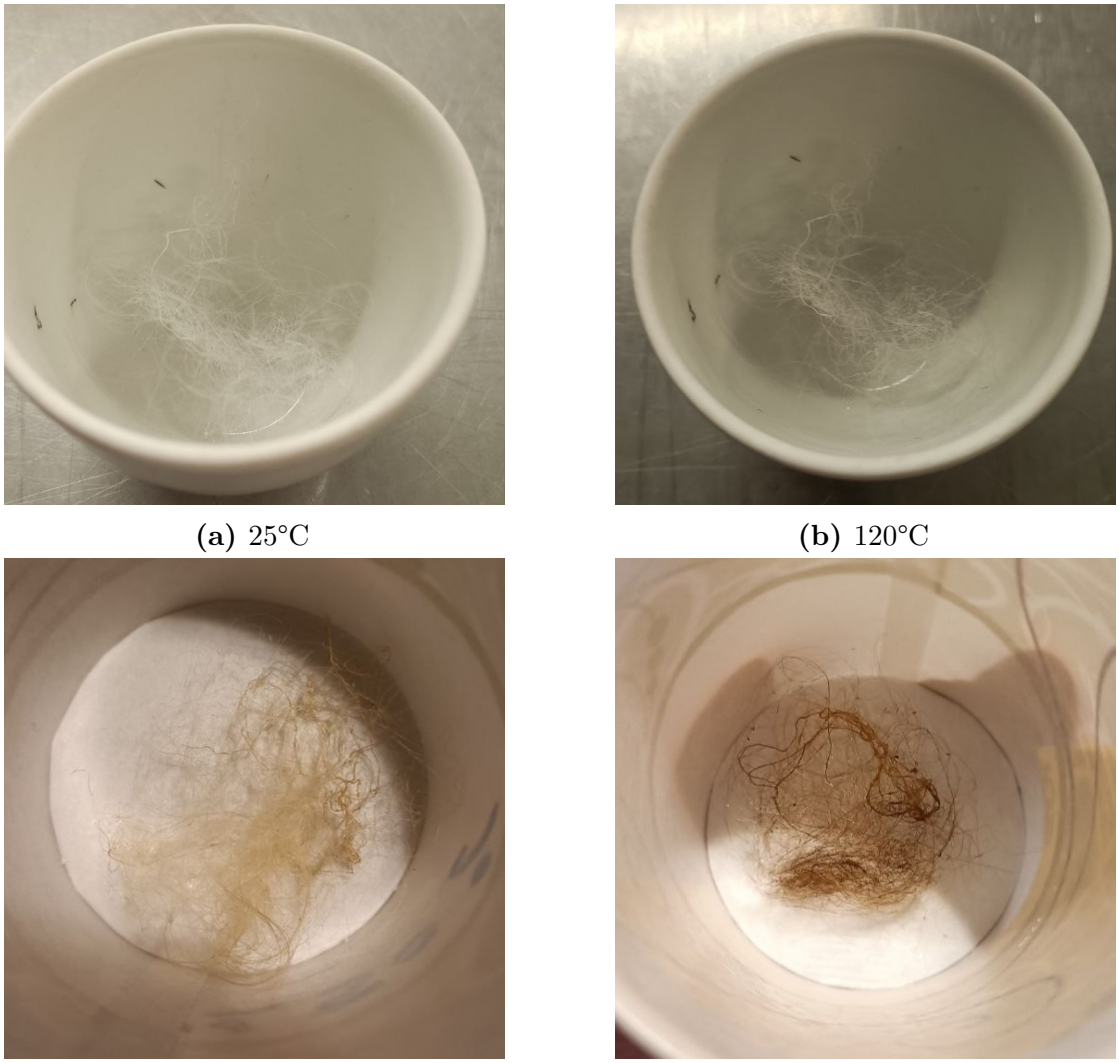

(a) 25°C **(b)** 120°C

(c) 135°C **(d)** 175°C

Figure G.2: How temperature influences the fibre aspect.

References

[1] Saptarshi Maiti, Md Rashedul Islam, Mohammad Abbas Uddin, Shaila Afroj, Stephen J. Eichhorn, and Nazmul Karim. «Sustainable Fiber-Reinforced Composites: A Review». In: *Advanced Sustainable Systems* 6.11 (2022), p. 2200258. DOI: https://doi.org/10.1002/adsu.202200258 (cit. on p. 1).

[2] Kotaro Kawajiri and Kaito Sakamoto. «Environmental impact of carbon fibers fabricated by an innovative manufacturing process on life cycle greenhouse gas emissions». In: *Sustainable Materials and Technologies* 31 (2022), e00365. ISSN: 2214-9937. DOI: https://doi.org/10.1016/j.susmat.2021.e00365 (cit. on p. 1).

[3] Jinchun Zhu, Huijun Zhu, James Njuguna, and Hrushikesh Abhyankar. «Recent Development of Flax Fibres and Their Reinforced Composites Based on Different Polymeric Matrices». In: *Materials* 6.11 (2013), pp. 5171–5198. ISSN: 1996-1944. URL: https://www.mdpi.com/1996-1944/6/11/5171 (cit. on pp. 1, 5, 10).

[4] Oleksandr Nechyporchuk, Mohamed Naceur Belgacem, and Julien Bras. «Production of cellulose nanofibrils: A review of recent advances». In: *Industrial Crops and Products* 93 (2016), pp. 2–25. ISSN: 0926-6690. DOI: https://doi.org/10.1016/j.indcrop.2016.02.016 (cit. on pp. 1, 12, 13).

[5] Karl M. O. Håkansson et al. «Hydrodynamic alignment and assembly of nanofibrils resulting in strong cellulose filaments». In: *Nature Communications* 5 (2014). URL: https://api.semanticscholar.org/CorpusID:16527237 (cit. on pp. 1, 12).

[6] Tsuguyuki Saito, Ryota Kuramae, Jakob Wohlert, Lars A. Berglund, and Akira Isogai. «An Ultrastrong Nanofibrillar Biomaterial: The Strength of Single Cellulose Nanofibrils Revealed via Sonication-Induced Fragmentation». In: *Biomacromolecules* 14.1 (2013). PMID: 23215584, pp. 248–253. DOI: 10.1021/bm301674e (cit. on p. 1).

[7] Mittal Nitesh et al. «Multiscale Control of Nanocellulose Assembly: Transferring Remarkable Nanoscale Fibril Mechanics to Macroscale Fibers». In: *ACS Nano* 12.7 (2018). PMID: 29741364, pp. 6378–6388. DOI: 10.1021/acsnano.8b01084 (cit. on pp. 2, 5, 13–15, 51).

[8] F.C. Campbell. «Chapter 1 - Introduction to Composite Materials and Processes: Unique Materials that Require Unique Processes». In: *Manufacturing Processes for Advanced Composites*. Ed. by F.C. Campbell. Amsterdam: Elsevier Science, 2004, pp. 1–37. ISBN: 978-1-85617-415-2. DOI: https://doi.org/10.1016/B978-185617415-2/50002-2 (cit. on p. 3).

[9] B. T. Åström. *Manufacturing of Polymer Composites*. Stockholm, Sweden: Chapman and Hall, 1997 (cit. on pp. 3, 5, 15–18, 21–24).

[10] Sunil Kumar Ramamoorthy, Mikael Skrifvars, and Anders Persson. «A Review of Natural Fibers Used in Biocomposites: Plant, Animal and Regenerated Cellulose Fibers». In: *Polymer Reviews* 55.1 (2015), pp. 107–162 (cit. on pp. 4, 6–8).

[11] Martina Wollerdorfer and Herbert Bader. «Influence of natural fibres on the mechanical properties of biodegradable polymers». In: *Industrial Crops and Products* 8.2 (1998), pp. 105–112. ISSN: 0926-6690. DOI: https://doi.org/10.1016/S0926-6690(97)10015-2 (cit. on p. 4).

[12] Mikaela Börjesson and Gunnar Westman. «Crystalline Nanocellulose — Preparation, Modification, and Properties». In: Jan. 2015, pp. 159–191. DOI: 10.5772/61899 (cit. on p. 6).

[13] «The Utilization of Vegetable Fibers in Cementitious Materials». In: *Encyclopedia of Renewable and Sustainable Materials*. Ed. by Saleem Hashmi and Imtiaz Ahmed Choudhury. Oxford: Elsevier, 2020, pp. 649–662. DOI: https://doi.org/10.1016/B978-0-12-803581-8.11596-6 (cit. on p. 6).

[14] C. Baley. «Analysis of the flax fibres tensile behaviour and analysis of the tensile stiffness increase». In: *Composites Part A: Applied Science and Manufacturing* 33.7 (2002), pp. 939–948. ISSN: 1359-835X. DOI: https://doi.org/10.1016/S1359-835X(02)00040-4 (cit. on pp. 6, 10, 11).

[15] Libo Yan, Nawawi Chouw, and Krishnan Jayaraman. «Flax fibre and its composites – A review». In: *Composites Part B: Engineering* 56 (2014), pp. 296–317. ISSN: 1359-8368. DOI: https://doi.org/10.1016/j.compositesb.2013.08.014 (cit. on pp. 6–9).

[16] Charlet K. Jernot J. P. Eve S. Gomina M. and Bréard J. «Multi-scale morphological characterisation of flax: From the stem to the fibrils.» In: *Carbohydrate Polymers* 82.1 (2010), pp. 54–61. DOI: https://doi.org/10.1016/J.CARBPOL.2010.04.022 (cit. on pp. 8, 9).

[17] K. Charlet, C. Baley, C. Morvan, J.P. Jernot, M. Gomina, and J. Bréard. «Characteristics of Hermès flax fibres as a function of their location in the stem and properties of the derived unidirectional composites». In: *Composites Part A: Applied Science and Manufacturing* 38.8 (2007), pp. 1912–1921. ISSN: 1359-835X. DOI: https://doi.org/10.1016/j.compositesa.2007.03.006 (cit. on pp. 9, 11).

[18] Sathish S. Prabhu L. Gokulkumar S. Karthi N. Balaji D. and Vigneshkumar N. «Extraction, Treatment and Applications of Natural Fibers for Bio-Composites – A Critical Review». In: *International Polymer Processing* 36.2 (2021), pp. 114–130. DOI: https://doi.org/10.1515/ipp-2020-4004 (cit. on p. 9).

[19] Avinash Pradip Manian, Michael Cordin, and Tung Pham. «Extraction of cellulose fibers from flax and hemp: a review». In: *Cellulose* 28 (2021), pp. 8275–8294 (cit. on p. 9).

[20] Edgars Spārniņs. «Mechanical properties of flax fibers and their composites». In: 2009 (cit. on p. 10).

[21] J George, ETJ Klompen, and Ton Peijs. «Thermal Degradation of Green and Upgraded Flax Fibres». In: *Advanced Composites Letters* 10 (Mar. 2001), pp. 81–88. DOI: 10.1177/096369350101000205 (cit. on p. 11).

[22] Masoodi Ryan, Elhajjar Rani, Pillai Krishna, and Sabo Ronald. «Mechanical characterization of cellulose nanofiber and bio-based epoxy composite». In: *Materials and Design* 36 (Apr. 2012), pp. 570–576. DOI: 10.1016/j.matdes.2011.11.042 (cit. on p. 11).

[23] Carter Nicklaus, Grant Isabelle, Dewey Marley, Bourque Mary, and David J. Neivandt. «Production and Characterization of Cellulose Nanofiber Slurries and Sheets for Biomedical Applications». In: *Frontiers in Nanotechnology* 3 (2021). DOI: 10.3389/fnano.2021.729743 (cit. on p. 12).

[24] Angeles Blanco, M. Concepcion Monte, Cristina Campano, Ana Balea, Noemi Merayo, and Carlos Negro. «Chapter 5 - Nanocellulose for Industrial Use: Cellulose Nanofibers (CNF), Cellulose Nanocrystals (CNC), and Bacterial Cellulose (BC)». In: *Handbook of Nanomaterials for Industrial Applications*. Ed. by Chaudhery Mustansar Hussain. Micro and Nano Technologies. Elsevier, 2018, pp. 74–126. ISBN: 978-0-12-813351-4. DOI: https://doi.org/10.1016/B978-0-12-813351-4.00005-5 (cit. on p. 12).

[25] A. Azammi, Ilyas R.A., S. Sapuan, Rushdan Ibrahim, Atikah Mahamud, Mochamad Asrofi, and A. Atiqah. «Characterization studies of biopolymeric matrix and cellulose fibres based composites related to functionalized fibre-matrix interface». In: Jan. 2020, pp. 29–93. ISBN: 9780081026656. DOI: 10.1016/B978-0-08-102665-6.00003-0 (cit. on p. 16).

[26] Darem Ahmad, Inge van den Boogaert, Jeremey Miller, Roy Presswell, and Hussam Jouhara. «Hydrophilic and hydrophobic materials and their applications». In: *Energy Sources, Part A: Recovery, Utilization, and Environmental Effects* 40.22 (2018), pp. 2686–2725. DOI: 10.1080/15567036.2018.1511642 (cit. on p. 16).

[27] V. Alvarez, A. Vazquez, and O. De La Osa. «Cyclic Water Absorption Behavior of Glass—Vinylester and Glass—Epoxy Composites». In: *Journal of Composite Materials* 41.10 (2007), pp. 1275–1289. DOI: 10.1177/0021998306067311 (cit. on pp. 18, 49).

[28] Omnexus. *Polyamide (PA) or Nylon: Complete Guide (PA6, PA66, PA11, PA12...)* URL: https://omnexus.specialchem.com/selection-guide/polyamide-pa-nylon (visited on 09/30/2023) (cit. on p. 18).

[29] K. Oksman, M. Skrifvars, and J.-F. Selin. «Natural fibres as reinforcement in polylactic acid (PLA) composites». In: *Composites Science and Technology* 63.9 (2003). Eco-Composites, pp. 1317–1324. ISSN: 0266-3538. URL: https://www.sciencedirect.com/science/article/pii/S0266353803001039 (cit. on pp. 18, 53).

[30] Omnexus. *Polylactide (PLA): Complete Guide to Accelerate your 'Green' Approach.* URL: https://omnexus.specialchem.com/selection-guide/polylactide-pla-bioplastic (visited on 09/30/2023) (cit. on p. 18).

[31] Ching Hao Lee, Abdan Khalina, and Seng Hua Lee. «Importance of Interfacial Adhesion Condition on Characterization of Plant-Fiber-Reinforced Polymer Composites: A Review». In: *Polymers* 13.3 (2021). ISSN: 2073-4360. DOI: 10.3390/polym13030438 (cit. on p. 19).

[32] Silu Huang, Qiuni Fu, Libo Yan, and Bohumil Kasal. «Characterization of interfacial properties between fibre and polymer matrix in composite materials – A critical review». In: *Journal of Materials Research and Technology* 13 (2021), pp. 1441–1484. ISSN: 2238-7854. DOI: https://doi.org/10.1016/j.jmrt.2021.05.076 (cit. on pp. 19, 25, 29).

[33] Yonghui Zhou, Mizi Fan, and Lihui Chen. «Interface and bonding mechanisms of plant fibre composites: An overview». In: *Composites Part B: Engineering* 101 (2016), pp. 31–45. ISSN: 1359-8368. DOI: https://doi.org/10.1016/j.compositesb.2016.06.055 (cit. on pp. 20, 52).

[34] Sabu Thomas Kuruvilla Joseph Sant Kumar Malhotra Koichi Goda and Meyyarappallil Sadasivan Sreekala, eds. *Polymer Composites*. Vol. 1. Lecture Notes in Statistics. Weinhein, Germany: Wiley-VCH, 2012 (cit. on p. 20).

[35] Pavle M. Spasojevic. «Chapter 15 - Thermal and Rheological Properties of Unsaturated Polyester Resins-Based Composites». In: *Unsaturated Polyester Resins*. Ed. by Sabu Thomas, Mahesh Hosur, and Cintil Jose Chirayil. Elsevier, 2019, pp. 367–406. ISBN: 978-0-12-816129-6. DOI: https://doi.org/10.1016/B978-0-12-816129-6.00015-6 (cit. on p. 21).

[36] Jingcheng Zeng. Dazhi Jiang Jinshui Yang Jiayu Xiao and Chaoyi Peng. «Compaction Behavior and Part Thickness Variation in Vacuum Infusion Molding Process». In: *Applied Composite Materials* 19.3 (2012), pp. 433–458. DOI: 10.1007/s10443-011-9217-8 (cit. on p. 22).

[37] Marco Gherlone. *Slide of Aeronautical structure course*. Turin, Italy, 2021 (cit. on p. 23).

[38] *ampliTex Art. No. 5057 data sheet*. Fribourg, Switzerland: Bcomp (cit. on pp. 27, 28, 39, 50).

[39] *HexPly® 6376 data sheet*. Stamford, Connecticut, U.S.A.: Hexcell (cit. on pp. 28, 39).

[40] *DION® 9100 data sheet*. Fredrikstad, Norway: REICHHOLD (cit. on pp. 28, 39).

[41] J.L. Ferracane and J.R. Condon. «Post-cure heat treatments for composites: properties and fractography». In: *Dental Materials* 8.5 (1992), pp. 290–295. ISSN: 0109-5641. DOI: https://doi.org/10.1016/0109-5641(92)90102-I (cit. on p. 33).

[42] D.K.Y. Tam, S. Ruan, P. Gao, and T. Yu. «10 - High-performance ballistic protection using polymer nanocomposites». In: *Advances in Military Textiles and Personal Equipment*. Ed. by E. Sparks. Woodhead Publishing Series in Textiles. Woodhead Publishing, 2012, pp. 213–237. DOI: https://doi.org/10.1533/9780857095572.2.213 (cit. on p. 38).

[43] Magnus Burman. *Fibre Composites Materials and Manufacturing*. Stockholm, Sweden, 2022 (cit. on p. 39).

[44] Suresh G Advani and E Murat Sozer. *Process Modeling in Composites Manufacturing*. New York and Basel: Marcel Dekker, 2003 (cit. on p. 54).